GEM TN-92-213

Report of the Task Force on a Hybrid Calorimeter

B. Worstell - Boston University
Hong Ma, Iuliu Stumer - Brookhaven National Laboratory
Xiaorong. Shi - California Institute of Technology
Yury Efremenko - Continuous Electron Bean Accelerator Facility
Alexandre Savin, Konstantine Shmakov - Oak Ridge National Laboratory
Paul M. Mockett - University of Washington

September 21, 1992

Abstract:

The task force was convened to address the option of building the GEM barrel calorimeter with a three layer structure: Liquid Krypton EM section; Liquid Argon hadronic section, thickness "a few" absorption lengths (we assume 0-3); and SPACAL hadronic section. The issues to be addressed in the geometry were its performance for: EM energy measurement, and leakage; electron-pion discrimination; missing ET measurements; and jet energy resolution. All as a function of varying the thickness of the liquid argon hadronic layer from zero to 3λ. The control for comparison purposes was the baseline 1, all-liquid-argon option.

GEM-TN-xxxx
9/21/92

REPORT OF THE TASK FORCE ON A HYBRID CALORIMETER

edited by
J. Womersley

Simulations performed by
Yu. Efremenko, A. Savin, and K. Shmakov

additional Task Force members:
H. Ma, P. Mockett, X. Shi, I Stumer, B. Worstell

AIM OF THE TASK FORCE

The task force was convened to address the option of building the GEM barrel calorimeter with a three layer structure, as below:

- Liquid Krypton EM section
- Liquid Argon hadronic section, thickness "a few" absorption lengths (we assumed 0—3)
- SPACAL hadronic section

The issues to be addressed in this geometry were its performance for:

- EM energy measurement, and leakage
- electron-pion discrimination
- missing ET measurements
- jet energy resolution

All as a function of varying the thickness of the liquid argon hadronic layer from zero to 3 λ. The control for comparison purposes was the baseline I, all-liquid-argon option.

INDIVIDUAL REPORTS

SEP 23 '92 19:12 FSUHEP 195 P02

SUMMARY

1.EM energy leakage

Savin has studied high energy EM shower leakage for 1 TeV electrons and photons. He has compared his results with those of Zeus and also of X. Shi for BaF_2. If no correction is made for leakage, then at these energies it will strongly damage the spectrum of energy response and reduce the number of events in the peak. However, a hadronic calorimeter with a relatively poor EM resolution (of even 40-80%/$\sqrt{E}$) is adequate to correct for energy lost and restore a Gaussian lineshape. This will work even with a relatively thick (2.8 X_0) cryostat wall behind the EM section. Alternatively, segmenting the last 1X_0 of the EM section separately can be used to correct for leakage. The proposed 8+17 X_0 front-back segmentation will not do the job of leakage corrections.

2. Electron-Pion discrimination

Yu. Efremenko has simulated electron-pion discrimination in Baseline I and hybrid geometries. The pion rejection is better in the LKr + SPACAL geometry by a factor of up to 2 (for 95% electron efficiency). For the 3 λ LAr hybrid the performance is similar to that of the baseline. The reason for this improved rejection is that the cryostat wall between the LKr section and the SPACAL absorbs the tails of EM showers, making them look more different from hadronic showers. So the extra discrimination would come at the expense of worsened resolution, and is probably not itself a good reason to go this route.

3. Missing E_T

K. Shmakov has studied missing E_T effects of energy loss fluctuations in cryostat walls. Events were generated in PYTHIA; GEANT was used to generate and parametrize individual shower energy loss distributions and then the parametrized distribution was sampled to obtain an E_T mismeasurement in each event. This was compared with the "irreducible" missing E_T due to neutrinos. The baseline I scheme has the best performance, followed by the hybrid with 1 λ LAr section, followed by LKr + SPACAL; but in all cases the missing E_T created by the cryostat walls is not significant compared with the irreducible E_T from neurtrinos.

4. Hadronic resolution

Efremenko has found that a study of how to weight the various layers in the calorimeter to achieve the best hadronic resolution yields very similar final resolutions for Baseline I, LKr+SPACAL and hybrid (with 3 λ LAr section). Since some weighting is unavoidable anyway (the various layers will unavoidably have different sampling fractions) this gives no reason to choose one geometry over another.

CONCLUSIONS

On the physics performance grounds studied, these simulations give no particular reason to prefer any one of the following designs over another:

Baseline I (LAr)
Hybrid (LKr + LAr + SPACAL)
LKr + SPACAL

Any of them would appear to be able to perform adequately; the extra cryostat walls have no terrible effects. It is suggested that the choice be made on grounds of cost, complexity or inherent performance (noise, constant term in resolution, calibratability) of the various technologies, which have not been looked at here.

SEP 23 '92 19:13 FSUHEP 195 P03

APPENDIX 1 — EM ENERGY LEAKAGE (A. Savin)

The simulated geometry is shown in Fig.1. The bulk mixture of the LKr/Pb E-M calorimeter was assumed to measure deposited energy with a resolution of $7.5/\sqrt{(E)} \oplus 0.4\%$. The bulk HC calorimeter is a mixture of Cu and plastic with an energy resolution of $40\%/\sqrt{(E)}$ or $80\%/\sqrt{(E)}$. The last few sections of the EM may be decared as 'dead' and excluded from the energy measurments. In this case the EM calorimeter became shorter, so these estimations are a little bit conservative. The table in Fig.2 shows different predictions of leakages for high energy EM showers. Zeus calculations are shown in Fig.3a, and Fig 3b shows X. Shi's calculations for barioum fluoride. For 1TeV electrons the leakage fluctuations are shown in Fig.4 (R.M.S and Gaussian fit sigma).

The other drawings are divided into groups labelled I-IV.

I - 1TeV electrons in 25.6X0 E-M calorimeter + 1.7X0 dead material
II - 1TeV electrons in 24.5X0 E-M calorimeter + 2.8X0 dead material
III - 1TeV photons in 25.6X0 E-M calorimeter + 1.7X0 dead material
IV - 1TeV photons in 24.5X0 E-M calorimeter + 2.8X0 dead material

In each group :

Fig.*-1 shows effect of leakage on resolution,
Fig.*-2 recovery of resolution by HC with $40\%/\sqrt{(E)}$
Fig.*-3 recovery of resolution by HC with $80\%/\sqrt{(E)}$
Fig.*-4 recovery of resolution by last 1X0 measurement (assumed perfect resolution)
Fig.*-5 shows correlation plot between energy deposit in EM calorimeter and fraction in first 8.54X0. Insufficient correlation for resolution improvement was obtained.

<u>Conclusions</u> :

1. Leakages for high energy electrons and photons strongly damage the spectrum of E-M calorimeter response.
2. Tails lead to loss of statistics as well as losses in the peak because of increased width. For photons the peak statistics go down as much as 35% (see Fig.III-1,2).
3. Leakage effects may be corrected by measurement of tail in HC with even a quite bad electromagnetic resolution ~ $40\text{-}80\%/\sqrt{(E)}$.
4. A separate readout of the last 1X0 would solve this problem equally well .
5. The proposed EM segmentation 8X0+17X0 is not effective for leakage corrections.

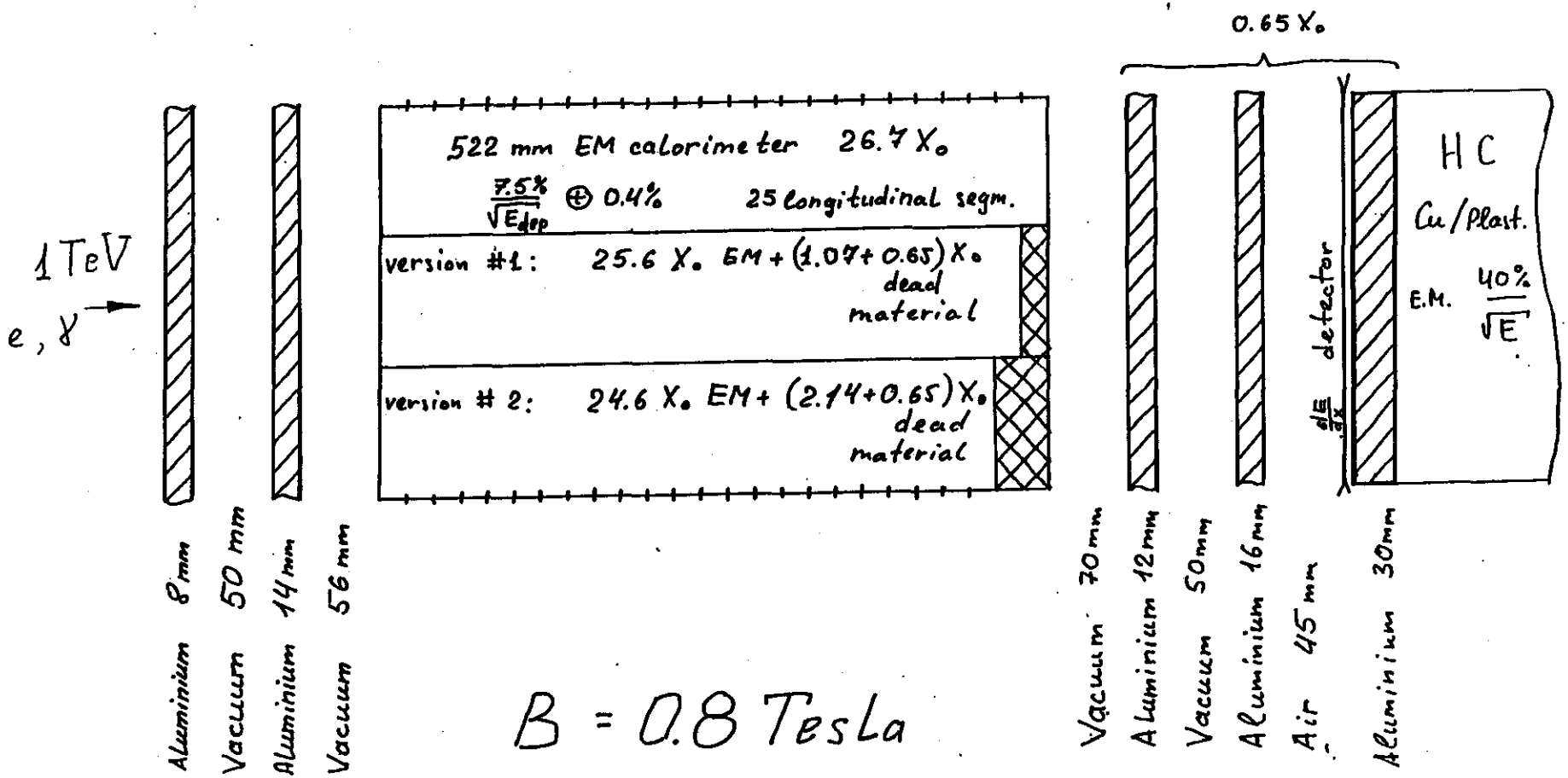
1 TeV
e, γ
Aluminium 8 mm
Vacuum 50 mm
Aluminium 14 mm
Vacuum 56 mm
522 mm EM calorimeter 26.7 X₀
7.5% / √E_dep ⊕ 0.4%
25 longitudinal segm.
version #1: 25.6 X₀ EM + (1.07+0.65) X₀ dead material
version # 2: 24.6 X₀ EM + (2.14+0.65) X₀ dead material
B = 0.8 Tesla
0.65 X₀
Vacuum 70 mm
Aluminium 12 mm
Vacuum 50 mm
Aluminium 16 mm
Air 45 mm
Aluminium 30 mm
dE/dx detector
HC
Cu/Plast.
E.M. 40% / √E

Fig. 1

E_leak after 25X0 to hadron calorimeter

Ein (TeV)	Iwata Eem leak	Rosenfeld tables 1988, >25 X0, Pb	Rosenfeld '86 Phys.Lett B170(1986) >25 X0, P	GEANT sim Leak > 25X0	
0.1	-	-	0.5%	0.6%	Y.Efremenko (Pb/LKr)
0.5	4.%	1.5 %	-	1.1%	X.Shi (BaF2)
1.0	6 %	2.0 %	1.5%	1.2%	A.Savin (Pb/LKr)
2.0	8 %	2.6 %	-		[25.6 X0]
4.0	-	3.4 %	-		
6.0	10 %	-	-		
8.0	-	4.2 %	-		
10.0	15 %	-	3.8%		

↑ ZEUS (90)

↑ Shmarokov ↑ Shmakov ↑ Efremenko

Fig 2

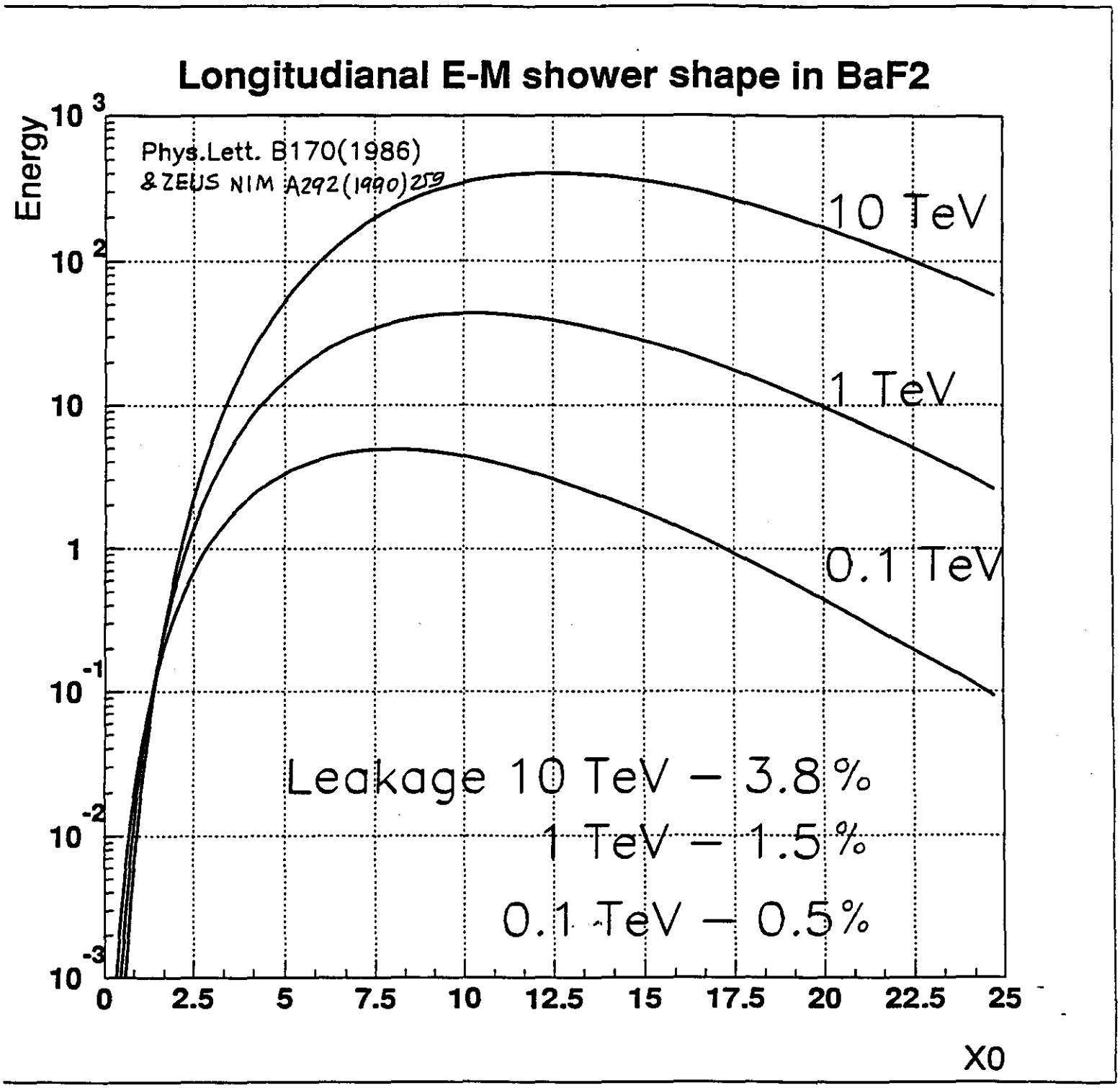

Yu. Efremenko

Fig 3a

X. SHI BaF_2
92/06/20 16.08

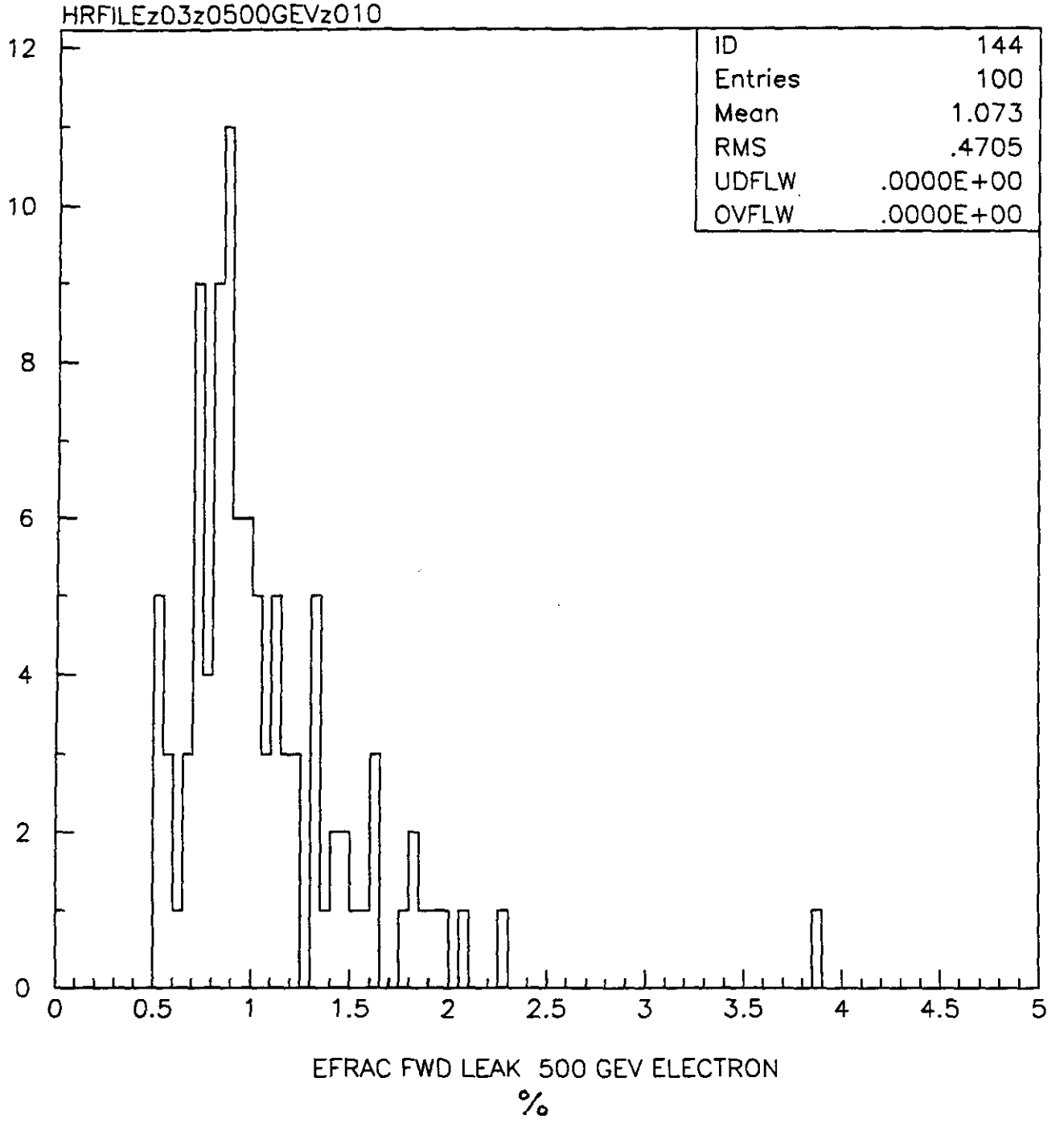

Fig. 3b.

Energy fluctuations

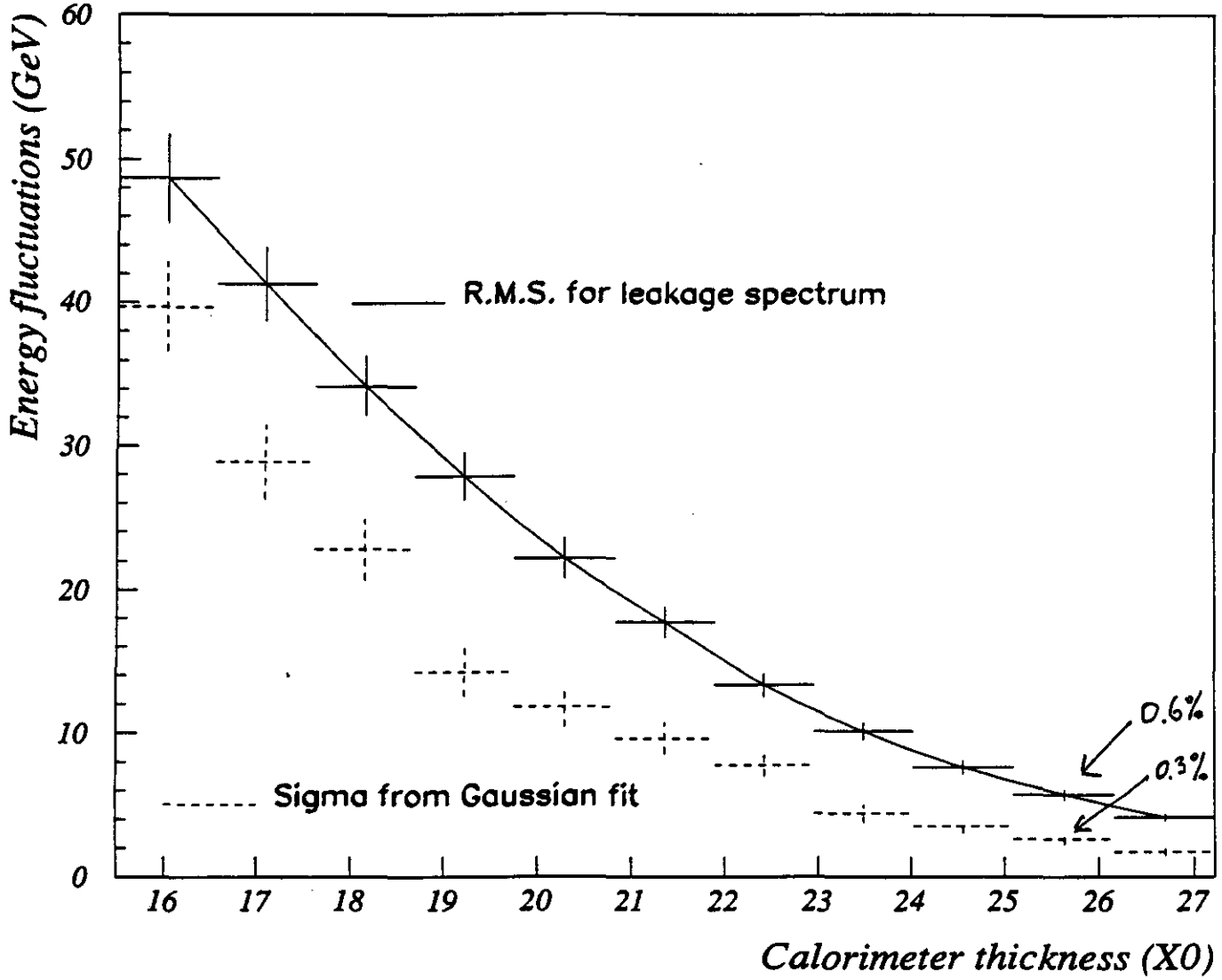

/A. Savin/

Fig 4

25.6 X0 E−M calorimeter

1.7 X0 dead material between E−M and Hadronic section

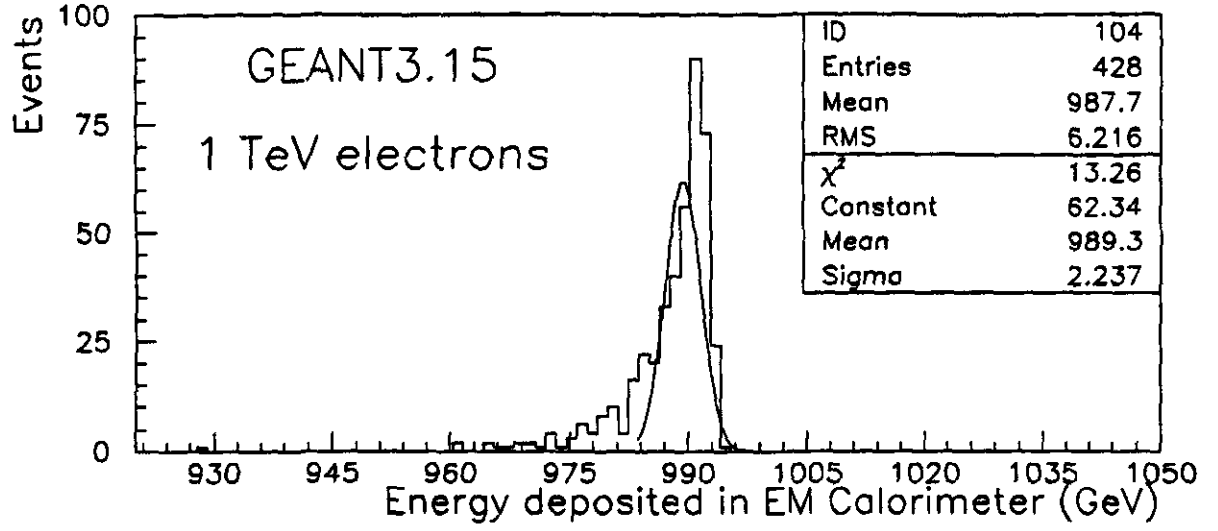

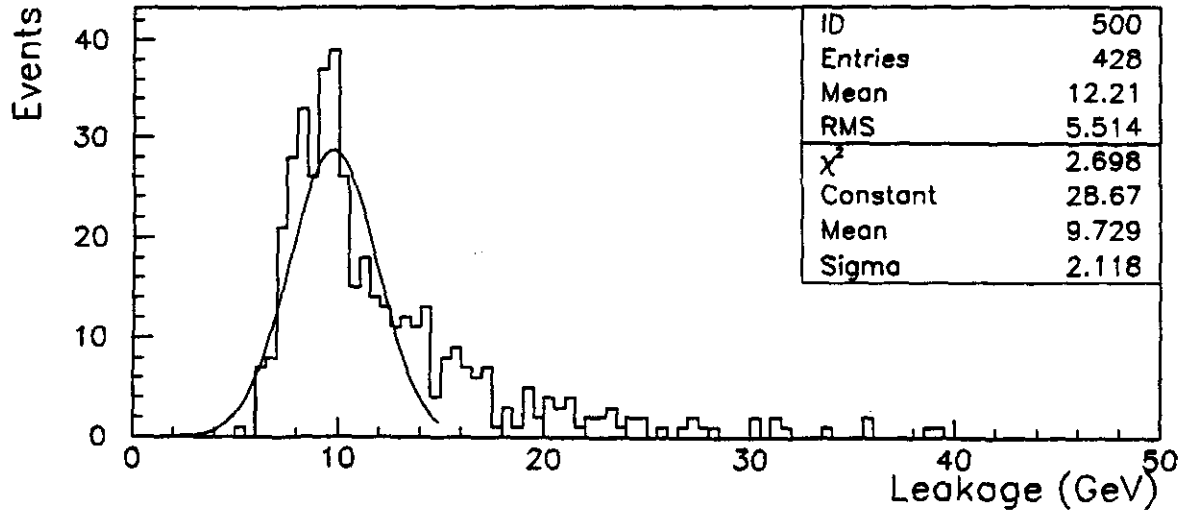

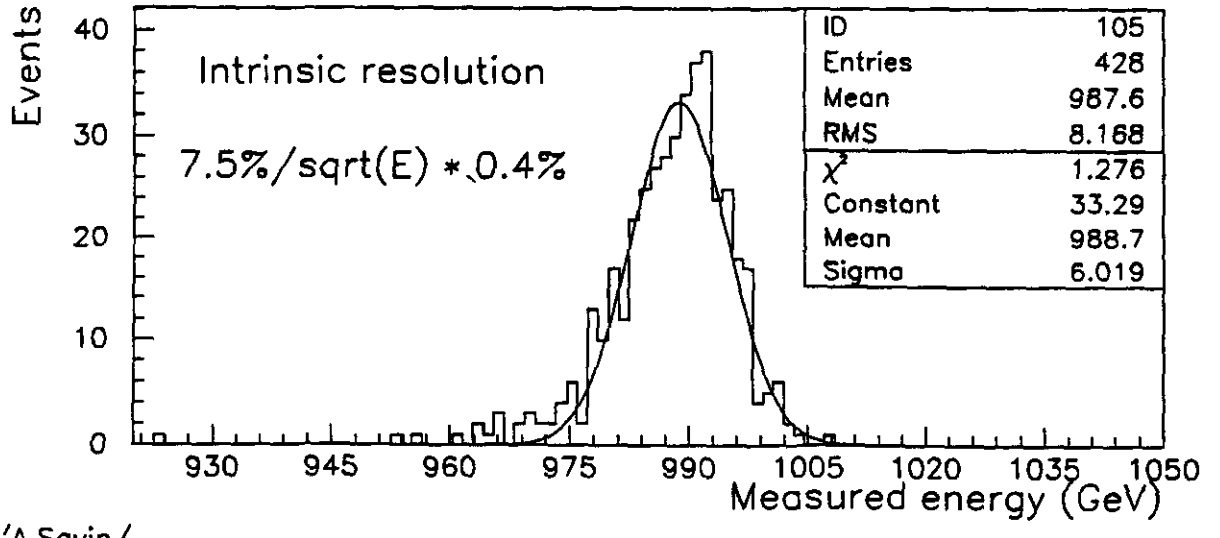

'A.Savin/

Fig. I-1

1.7 X0 dead material between E−M and Hadronic section

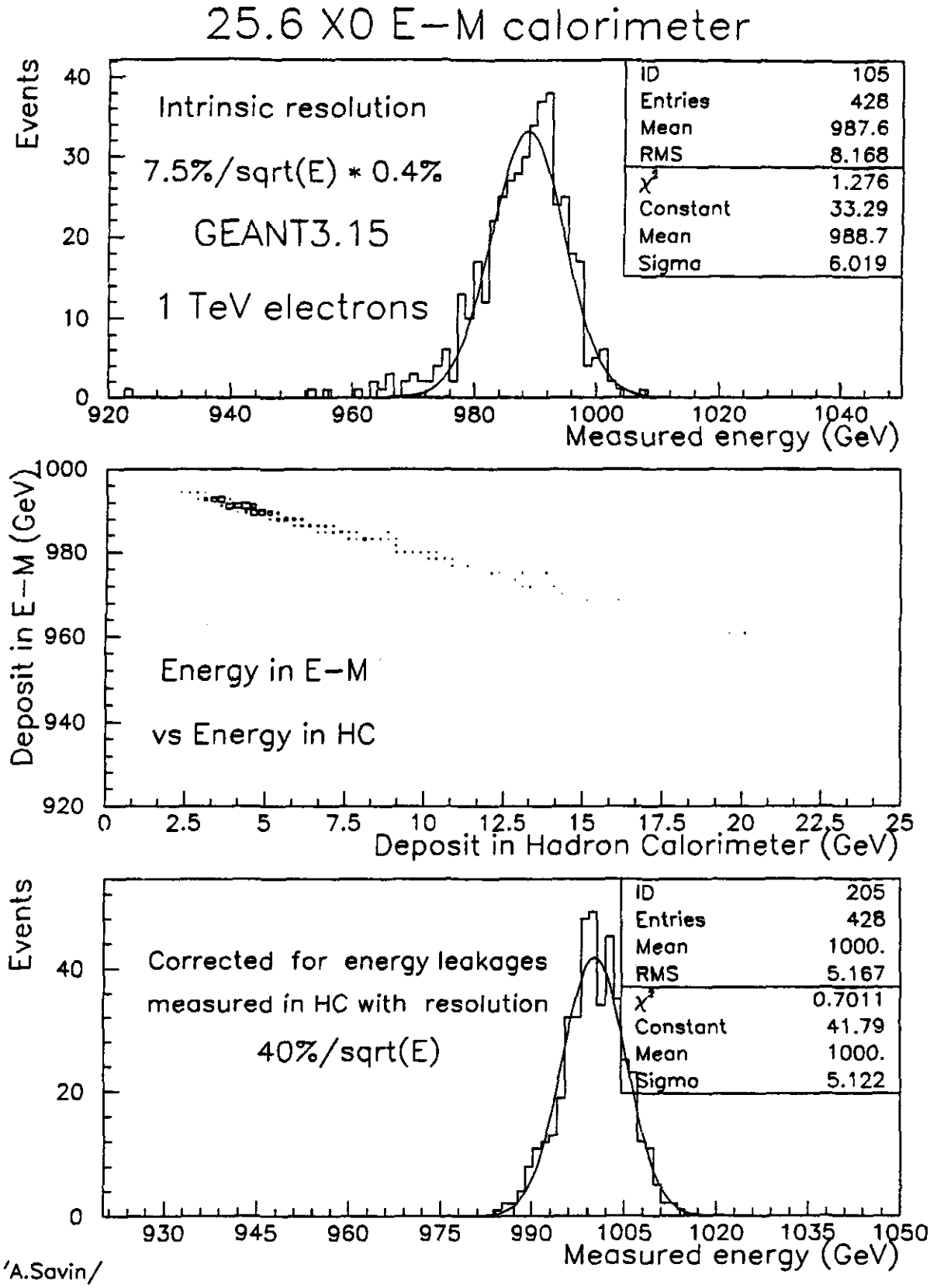

Fig I-2

25.6 X0 E−M calorimeter

1.7 X0 dead material between E−M and Hadronic section

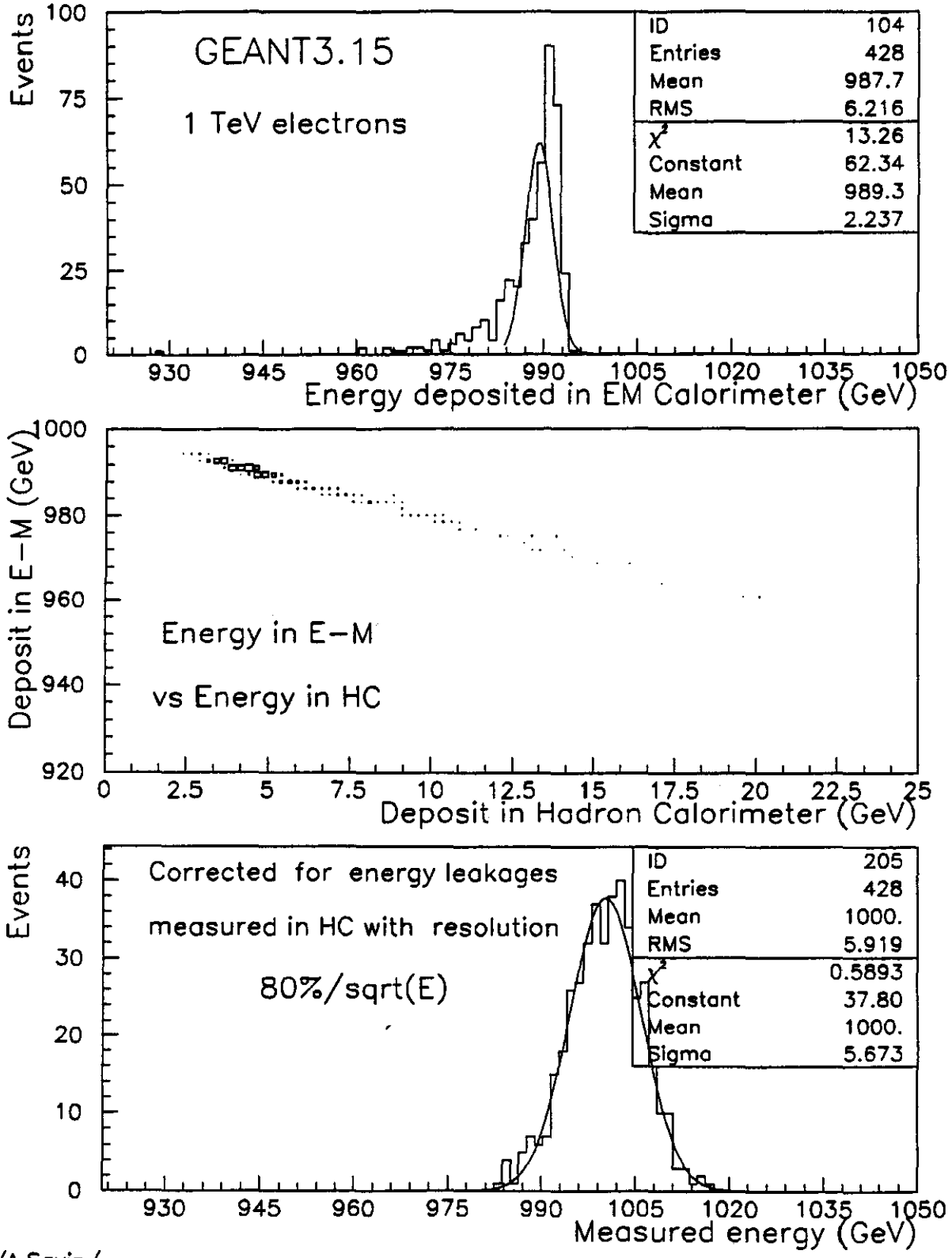

'A.Savin/

Fig I-3

25.6 X0 E−M calorimeter

1.7 X0 dead material between E−M and Hadronic section

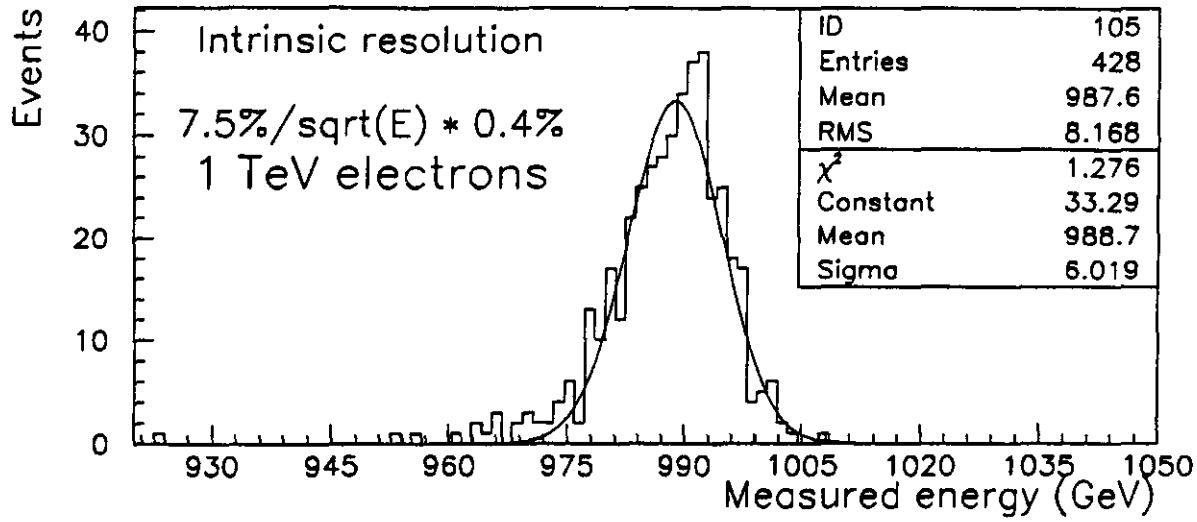

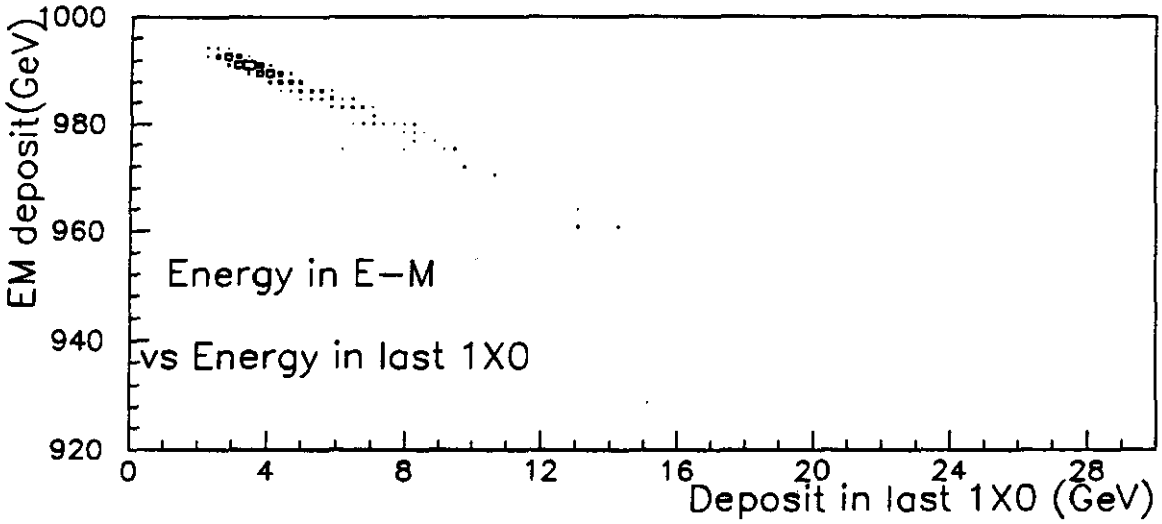

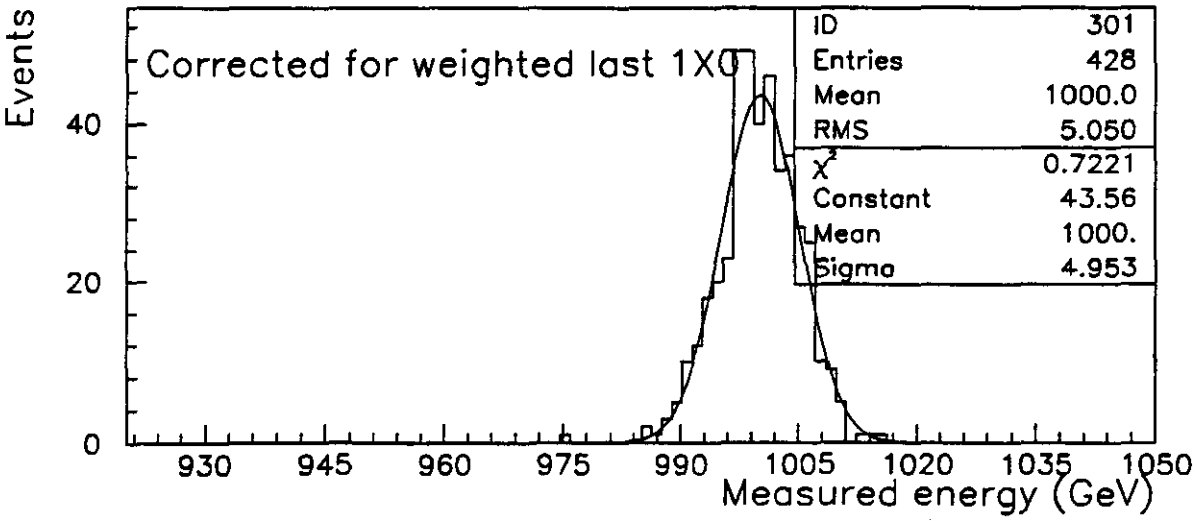

Fig I-4

Front section 8X0

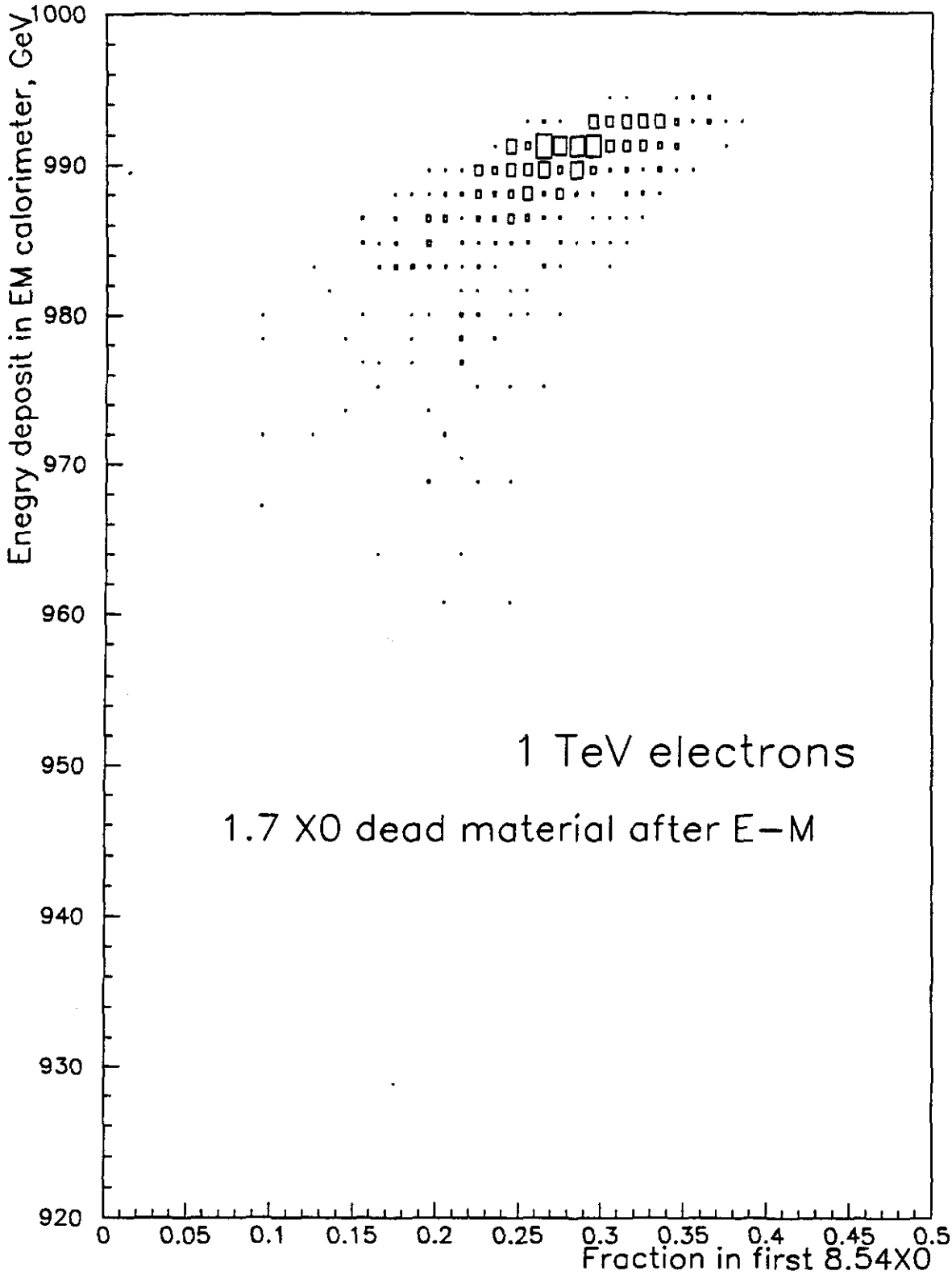

'A.Savin/

Fig I-5

24.5 X0 E−M calorimeter

2.8 X0 dead material between E−M and Hadronic section

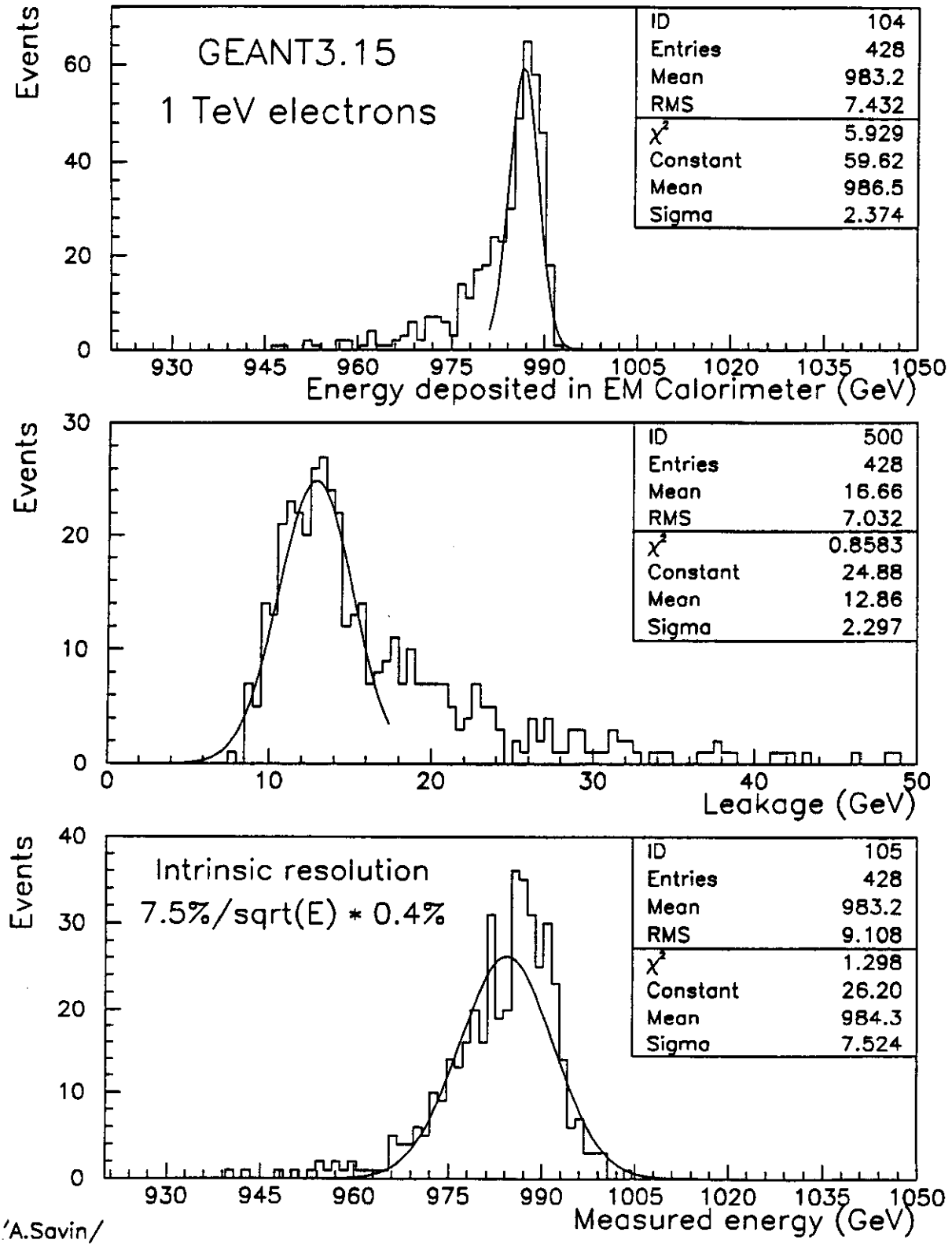

Fig II-1

2.8 X0 dead material between E−M and Hadronic section

24.5 X0 E−M calorimeter

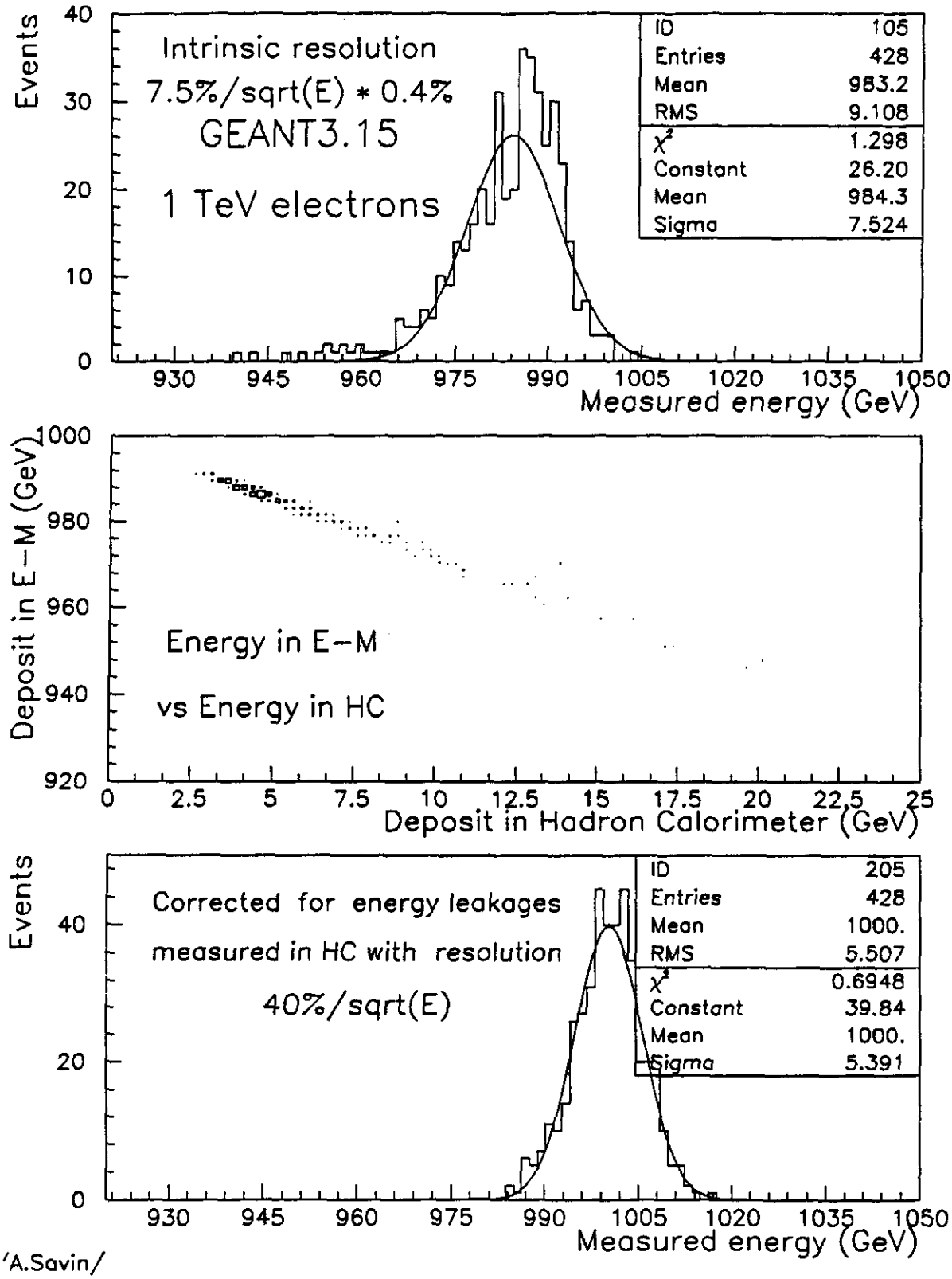

'A.Savin/

Fig II-2

24.5 X0 E−M calorimeter

2.8 X0 dead material between E−M and Hadronic section

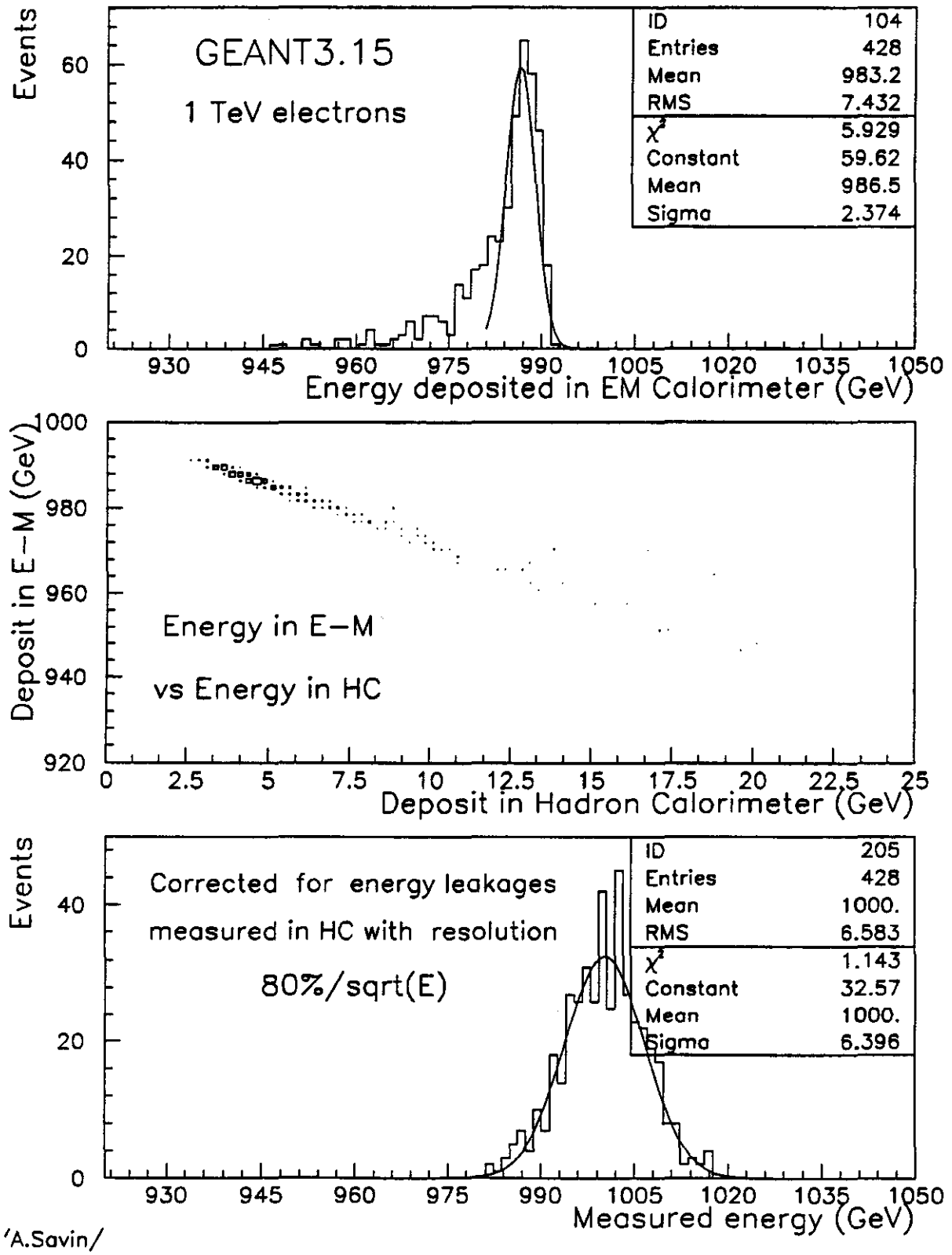

'A.Savin/

Fig II-3

24.5 X0 E−M calorimeter

2.8 X0 dead material between E−M and Hadronic section

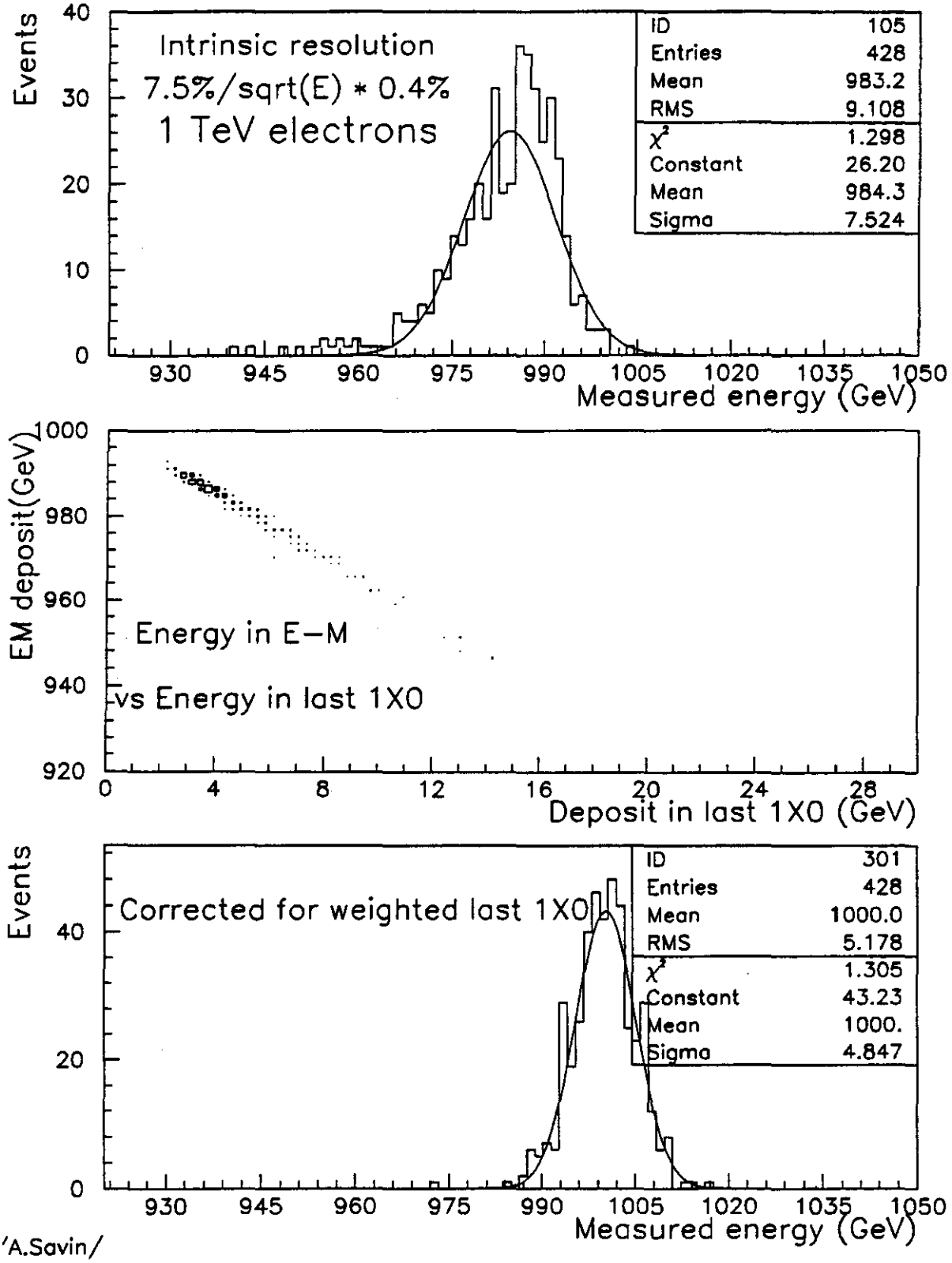

'A.Savin/

Fig II-4

Front section 8X0

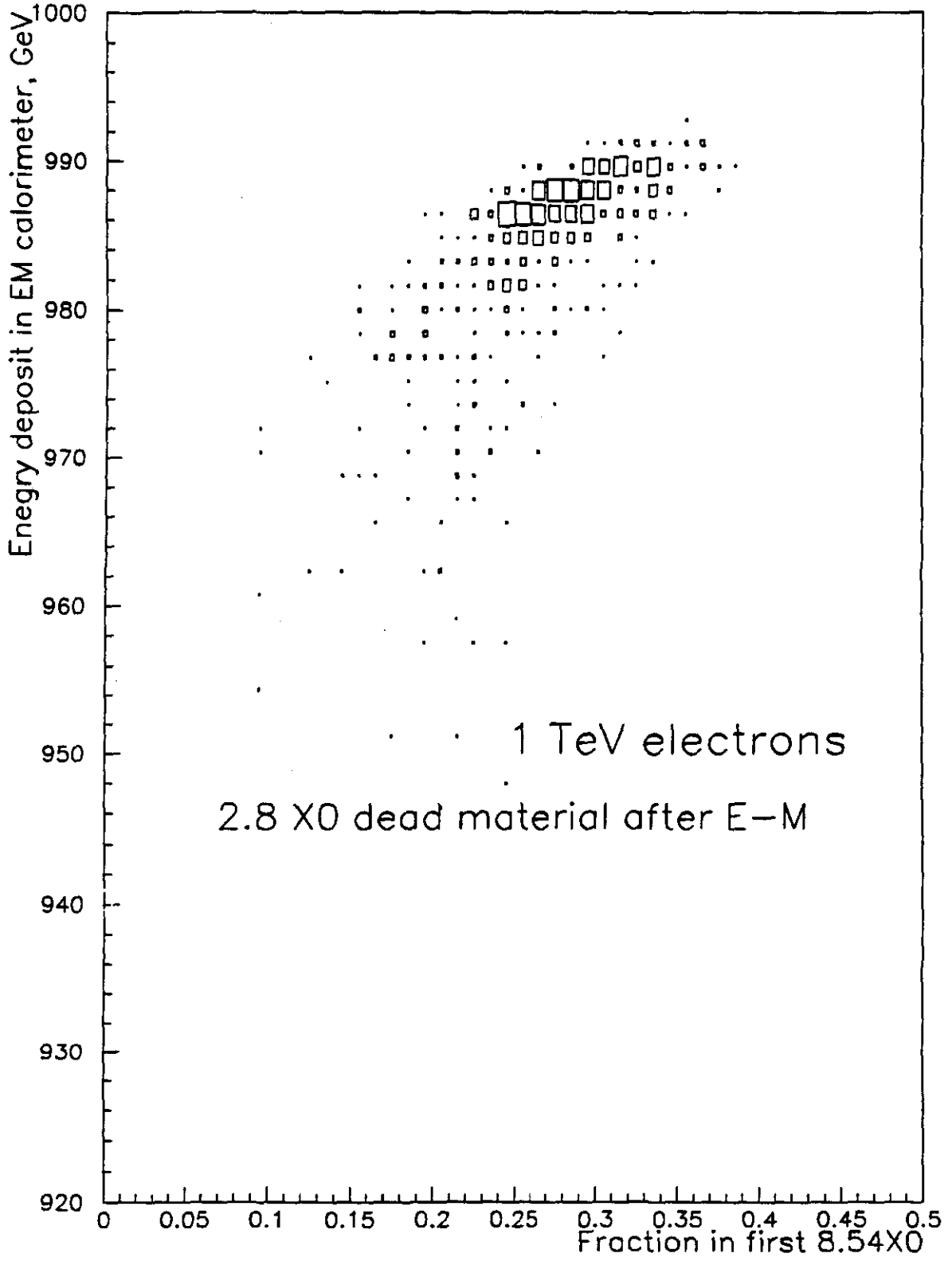

'A.Savin/

Fig II-5

25.6 X0 E−M calorimeter

1.7 X0 dead material between E−M and Hadronic section

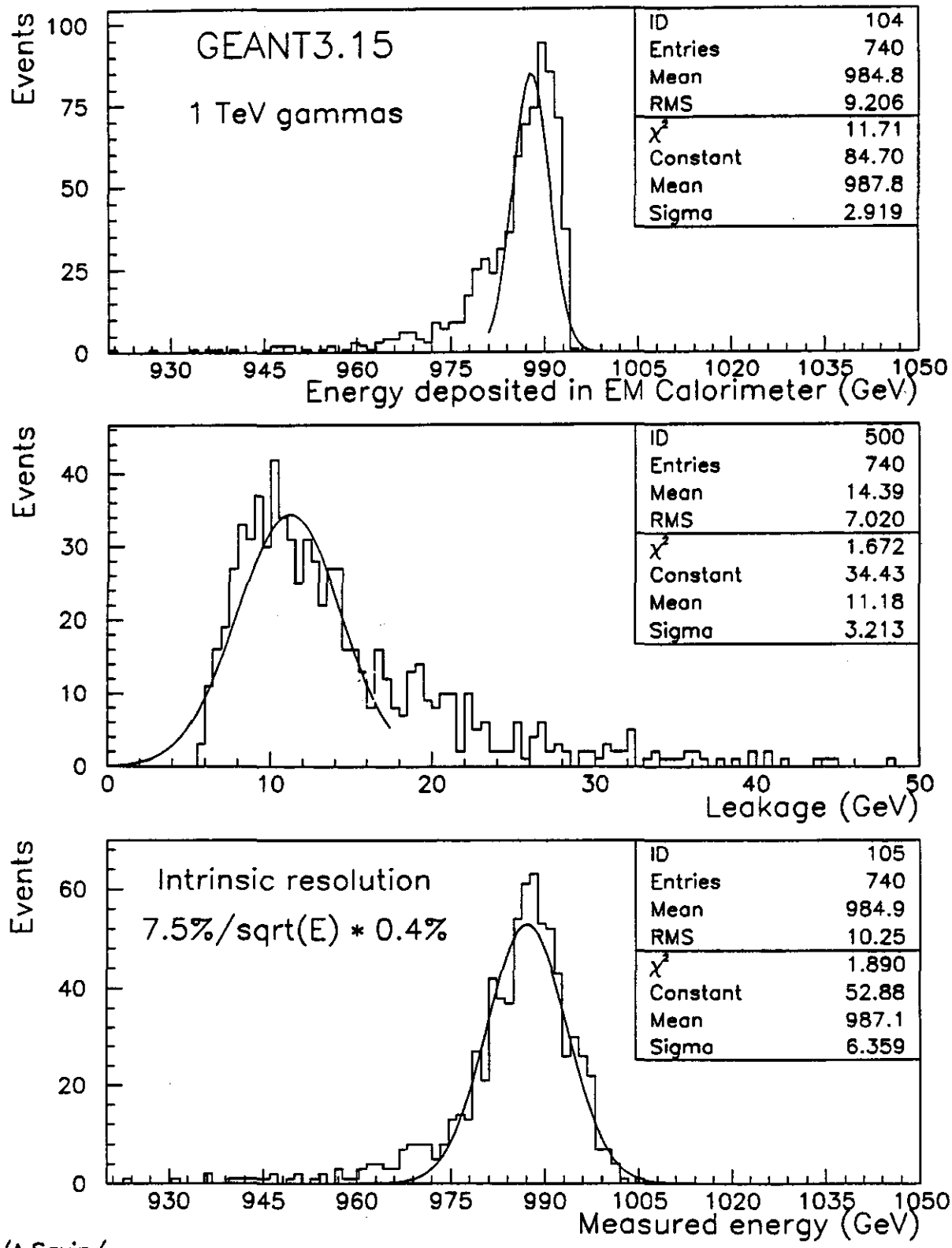

'A.Savin/

Fig III - 1

1.7 X0 dead material between E−M and Hadronic section

25.6 X0 E−M calorimeter

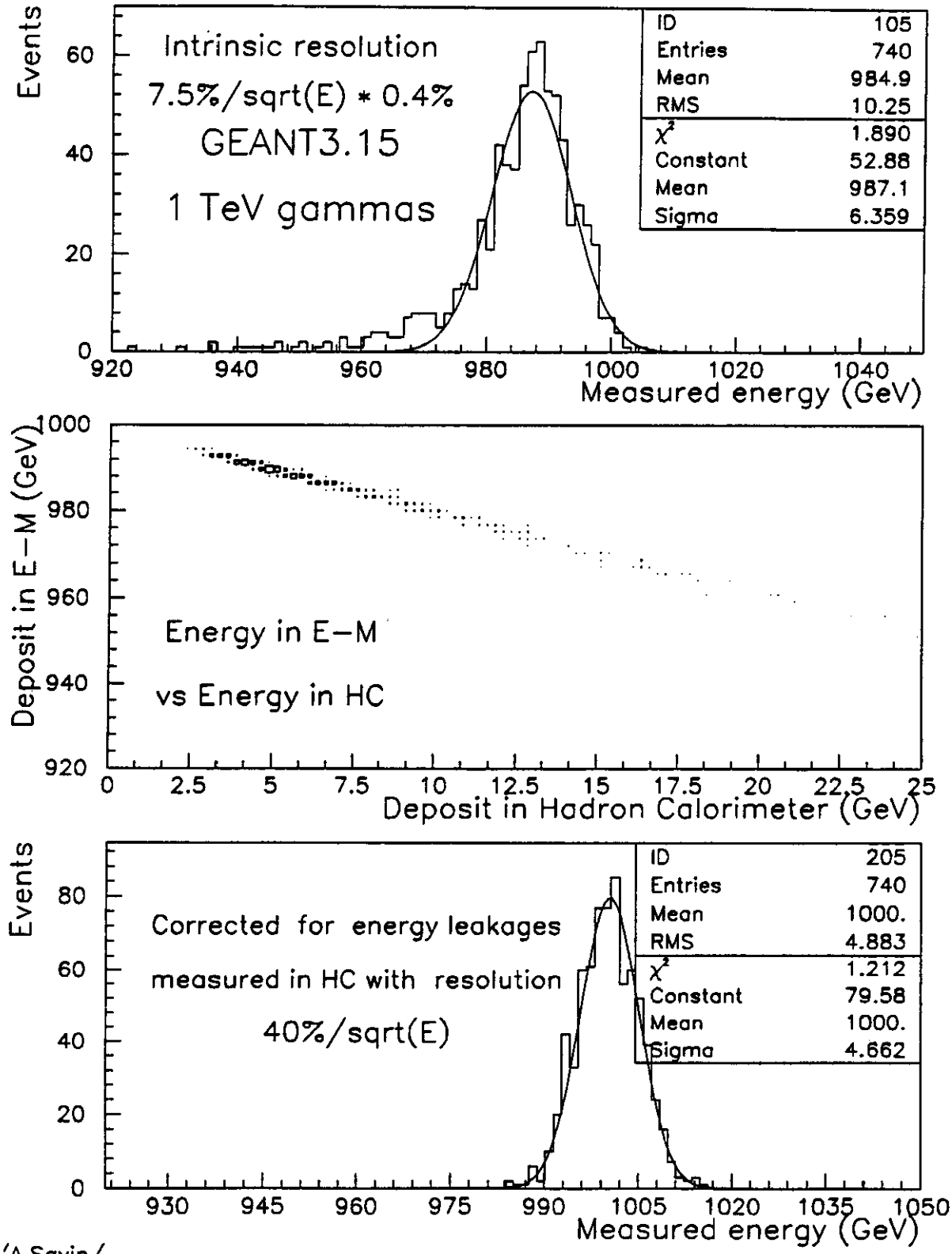

'A.Savin/

Fig III-2

25.6 X0 E−M calorimeter

1.7 X0 dead material between E−M and Hadronic section

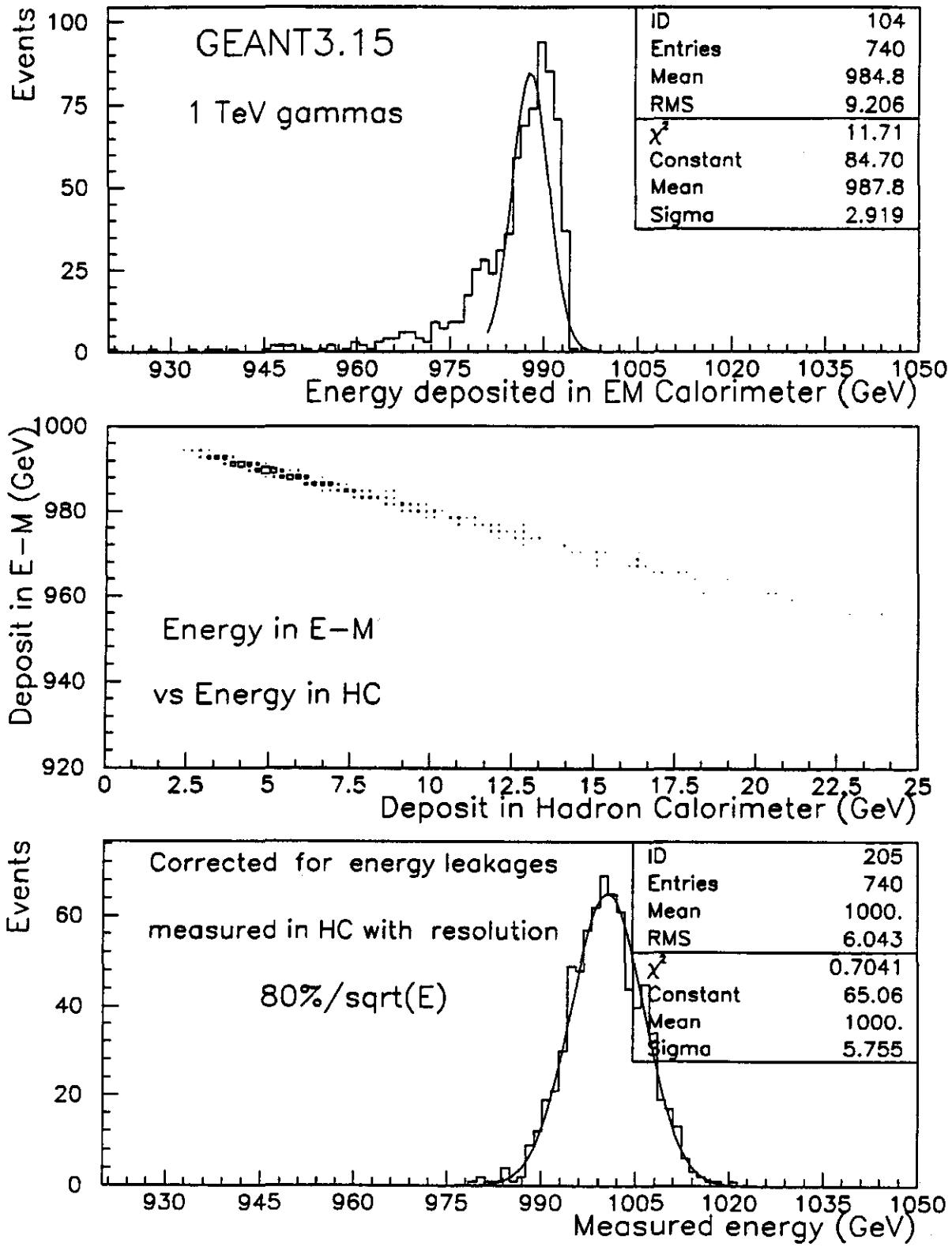

'A.Savin/

Fig III-3

25.6 X0 E−M calorimeter

1.7 X0 dead material between E−M and Hadronic section

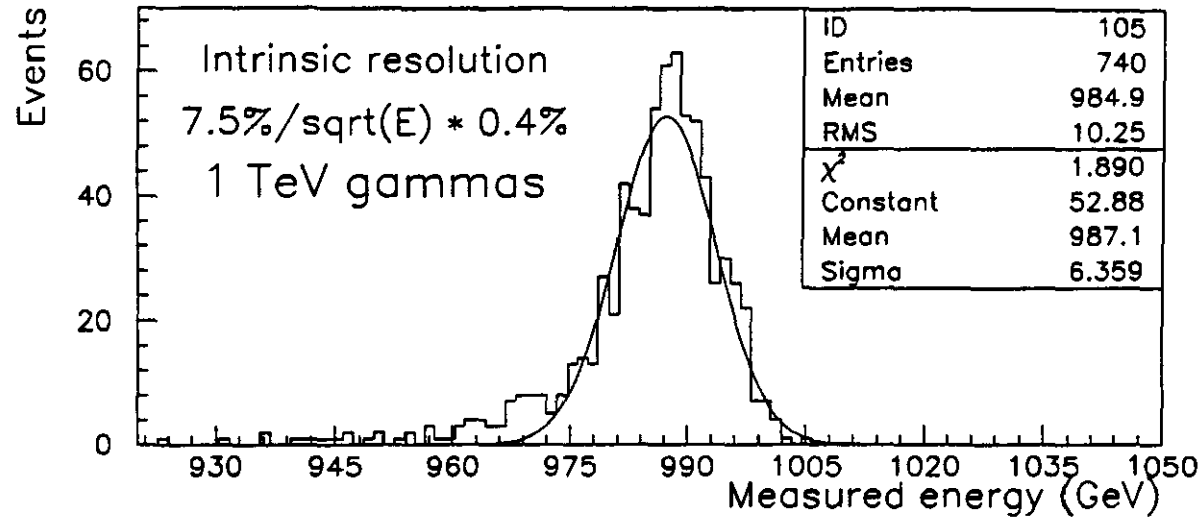

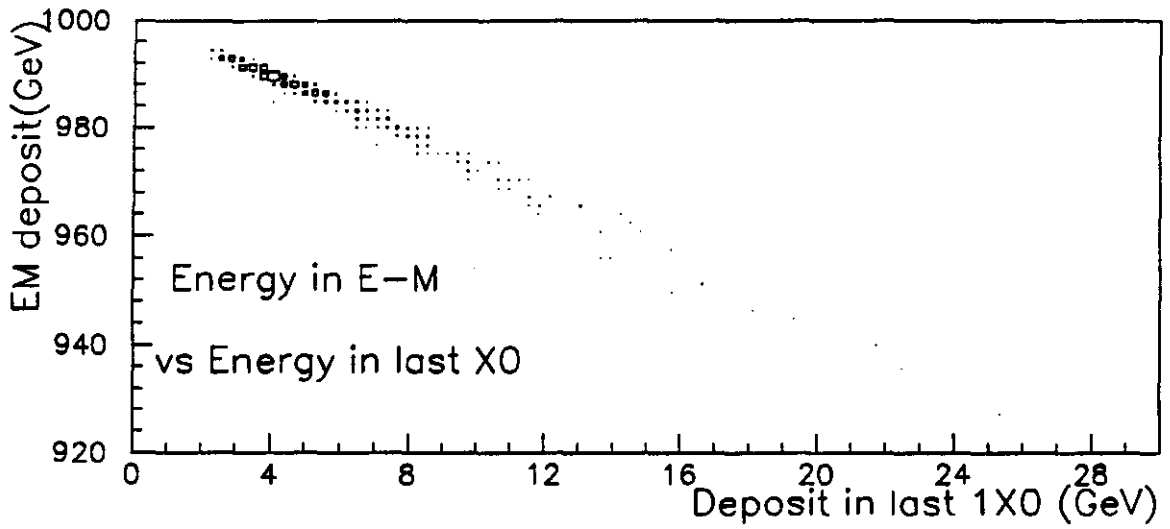

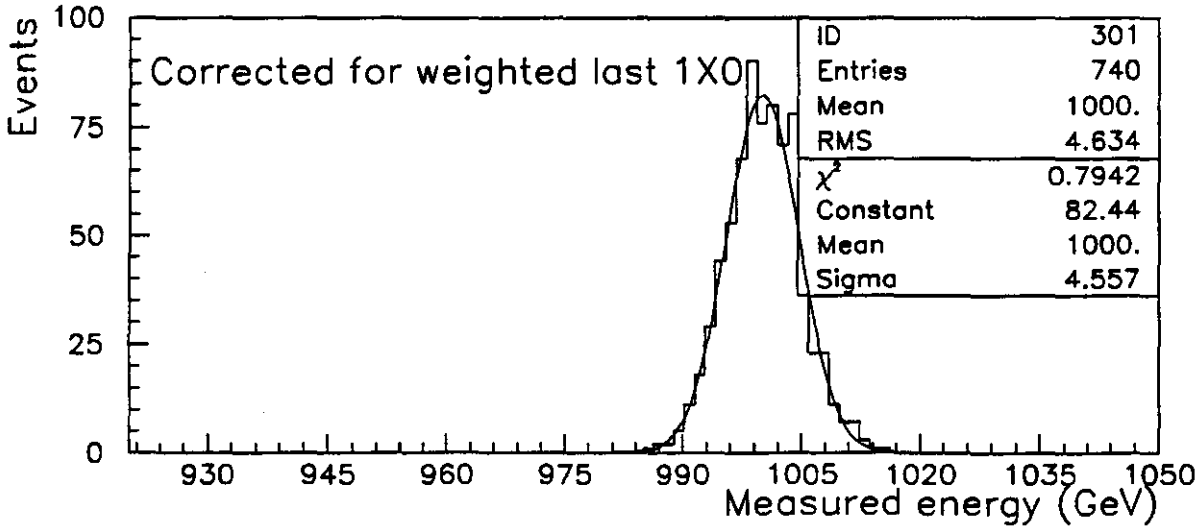

'A.Savin/

Fig III-4

Front section 8X0

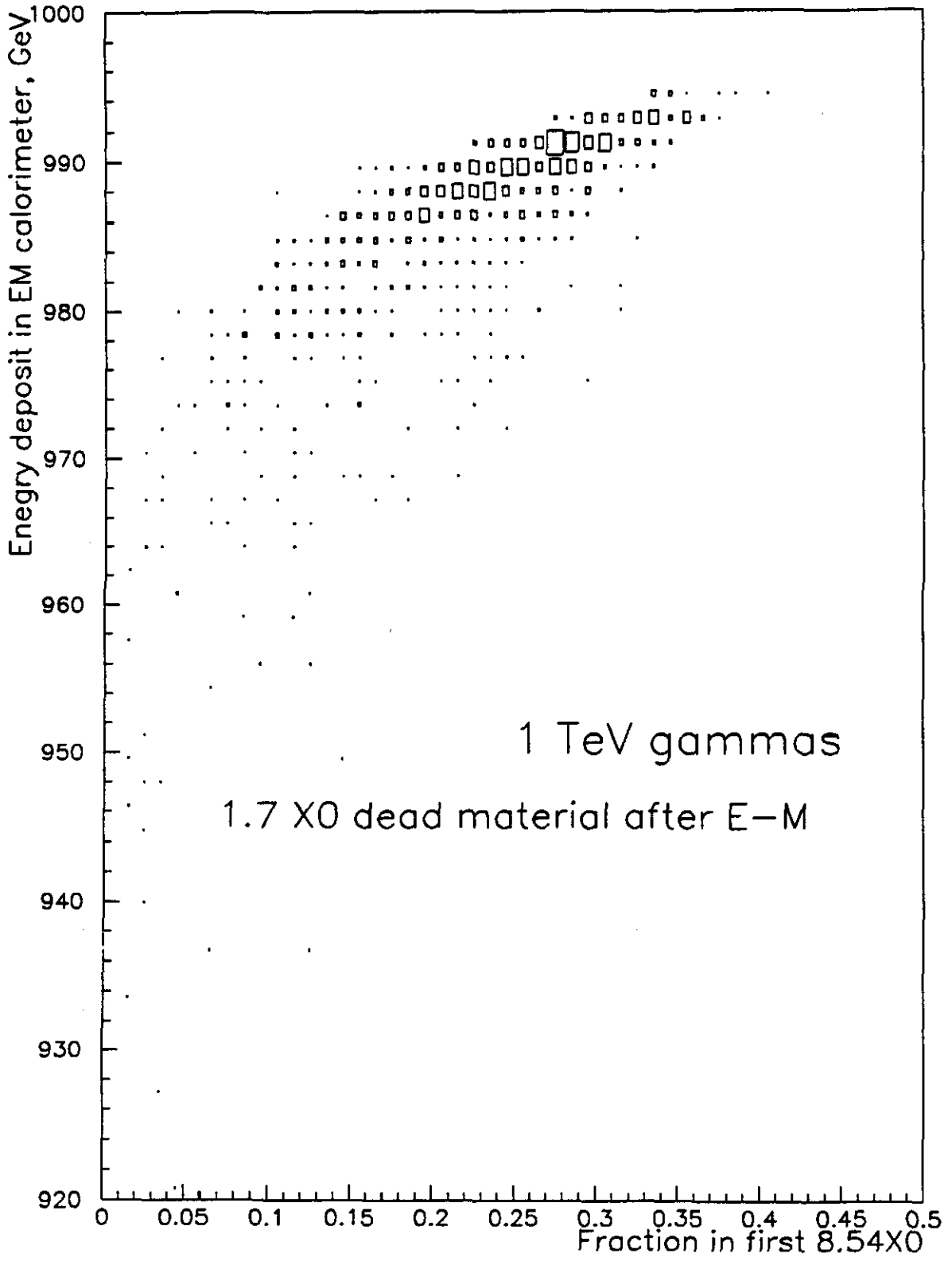

'A.Savin/

Fig III-5

24.5 X0 E−M calorimeter

2.8 X0 dead material between E−M and Hadronic section

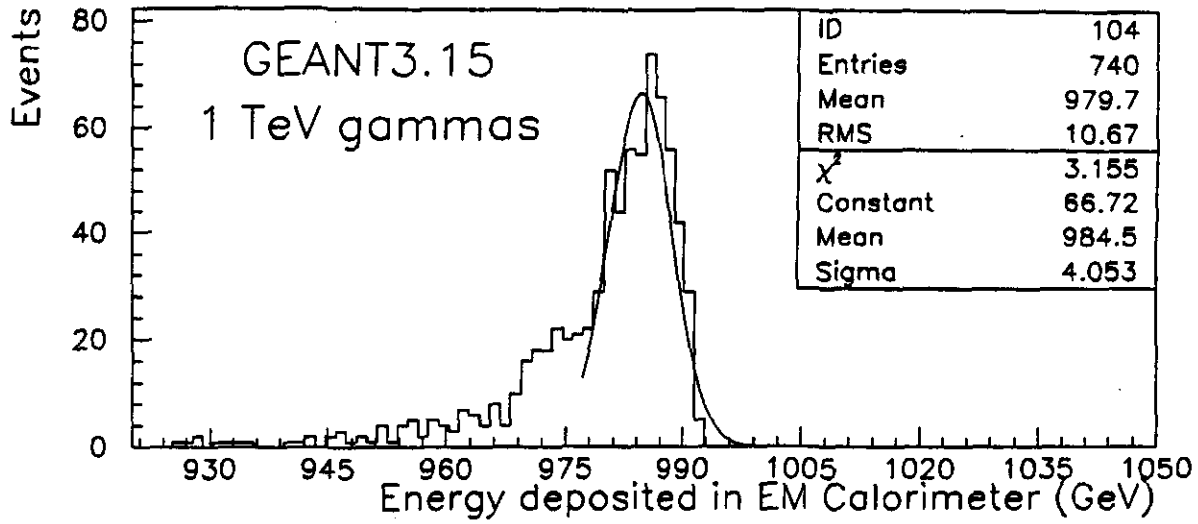

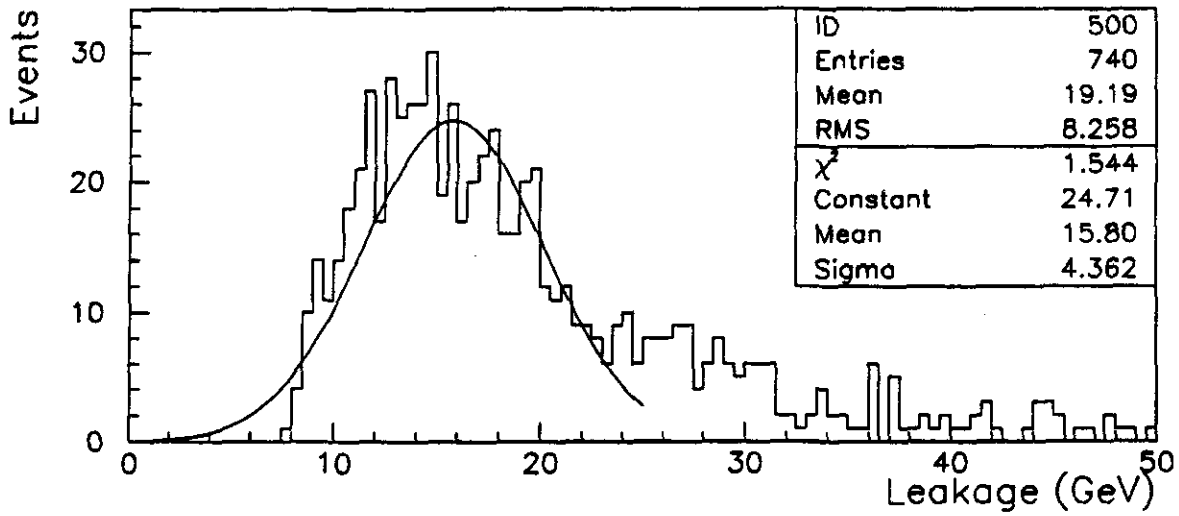

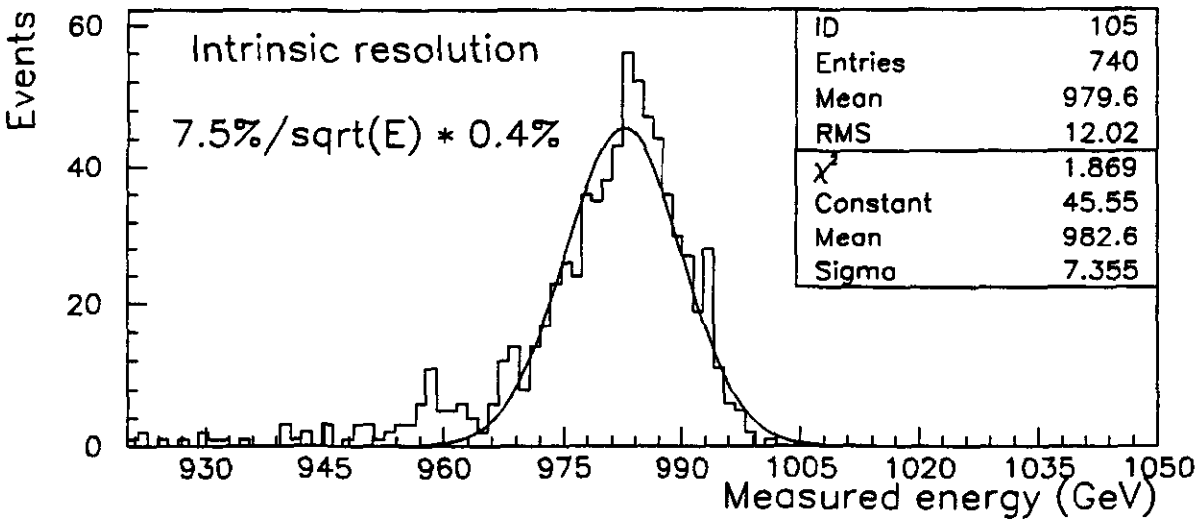

'A.Savin/

Fig IV-1

2.8 X0 dead material between E−M and Hadronic section

24.5 X0 E−M calorimeter

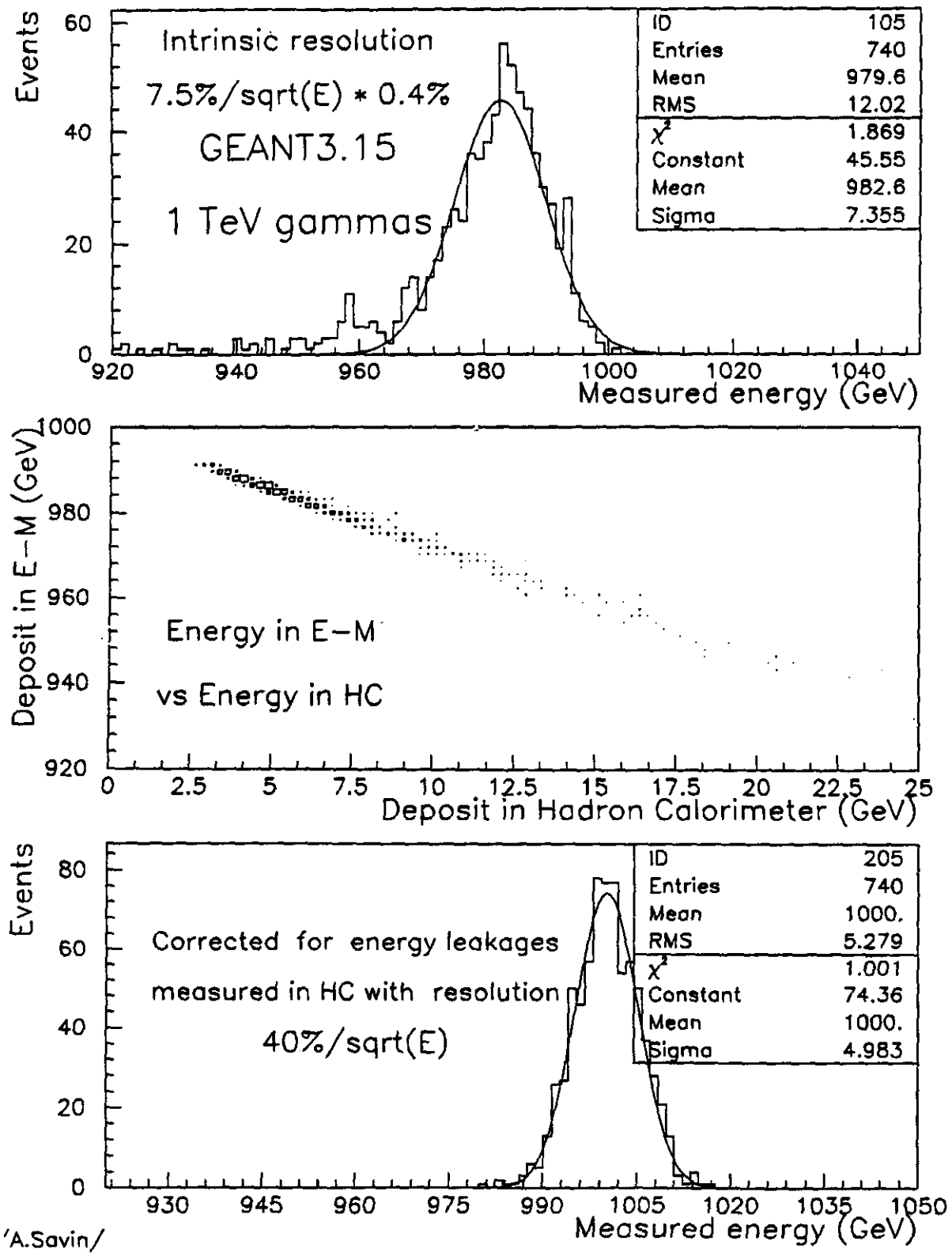

'A.Savin/

Fig IV-2

24.5 X0 E−M calorimeter

2.8 X0 dead material between E−M and Hadronic section

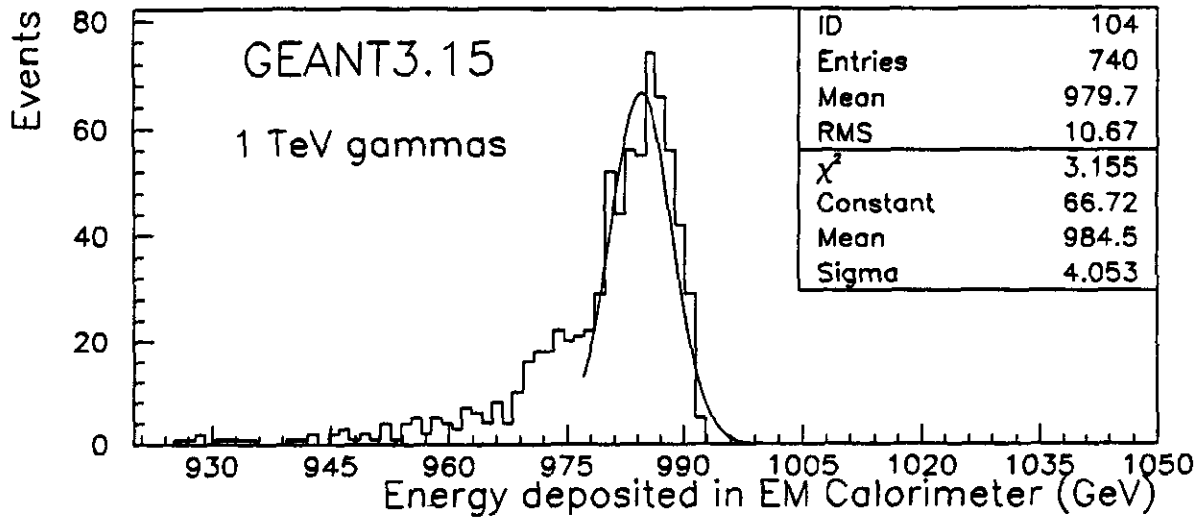

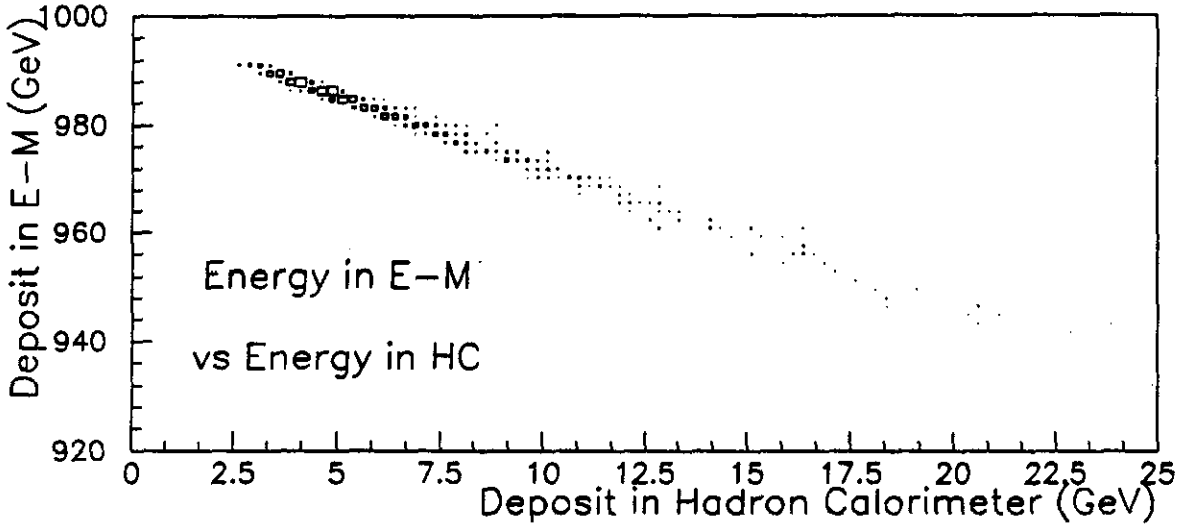

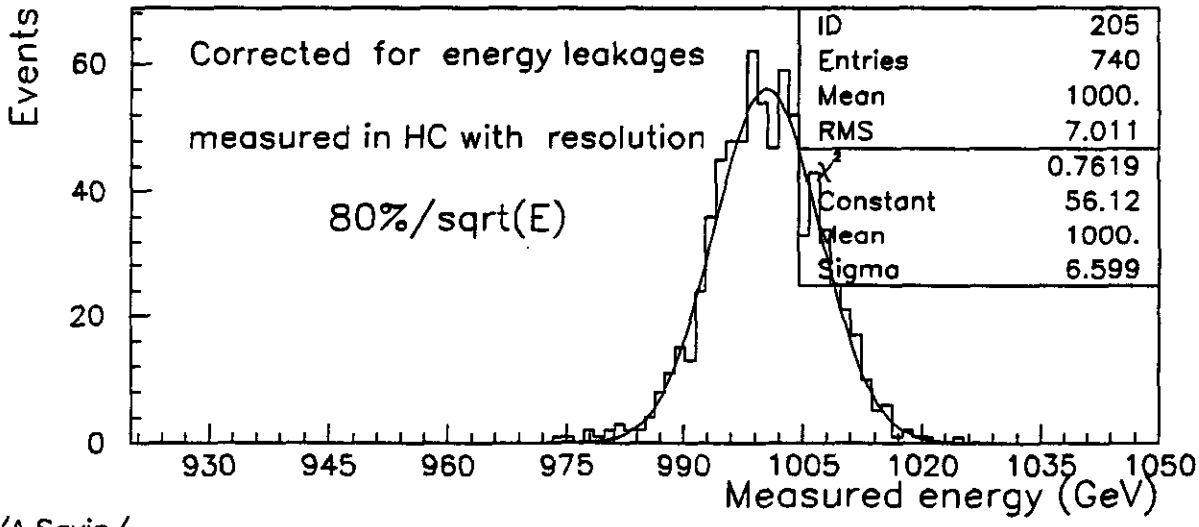

'A.Savin/

Fig. IV-3

24.5 X0 E−M calorimeter

2.8 X0 dead material between E−M and Hadronic section

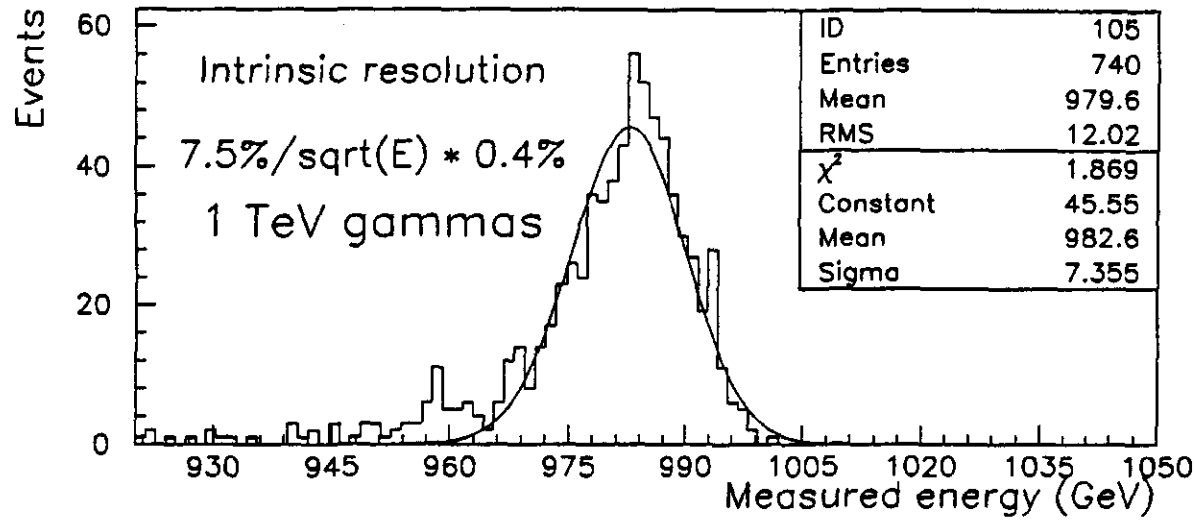

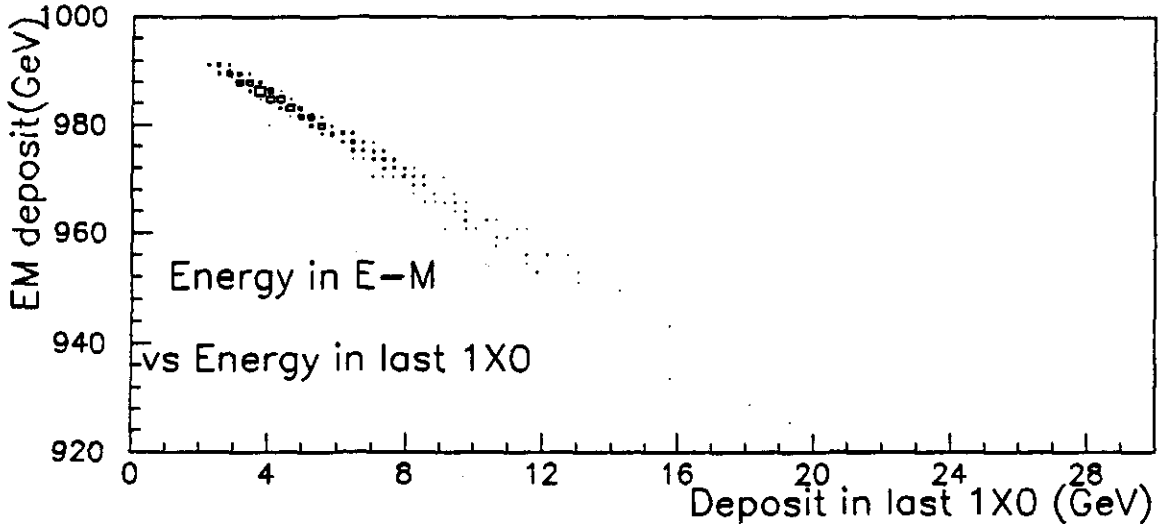

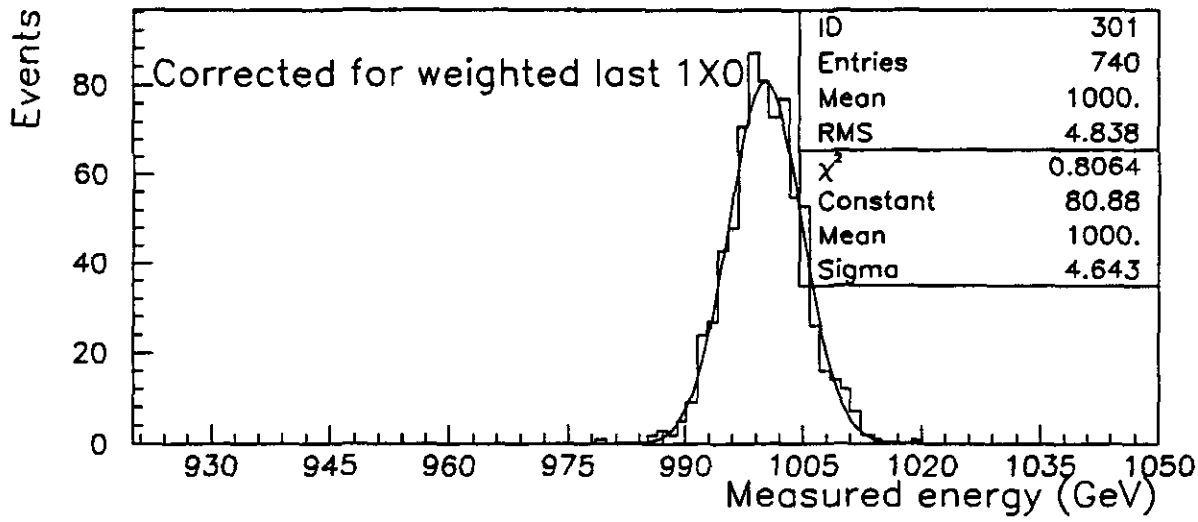

'A.Savin/

Fig IV-4

Front section 8X0

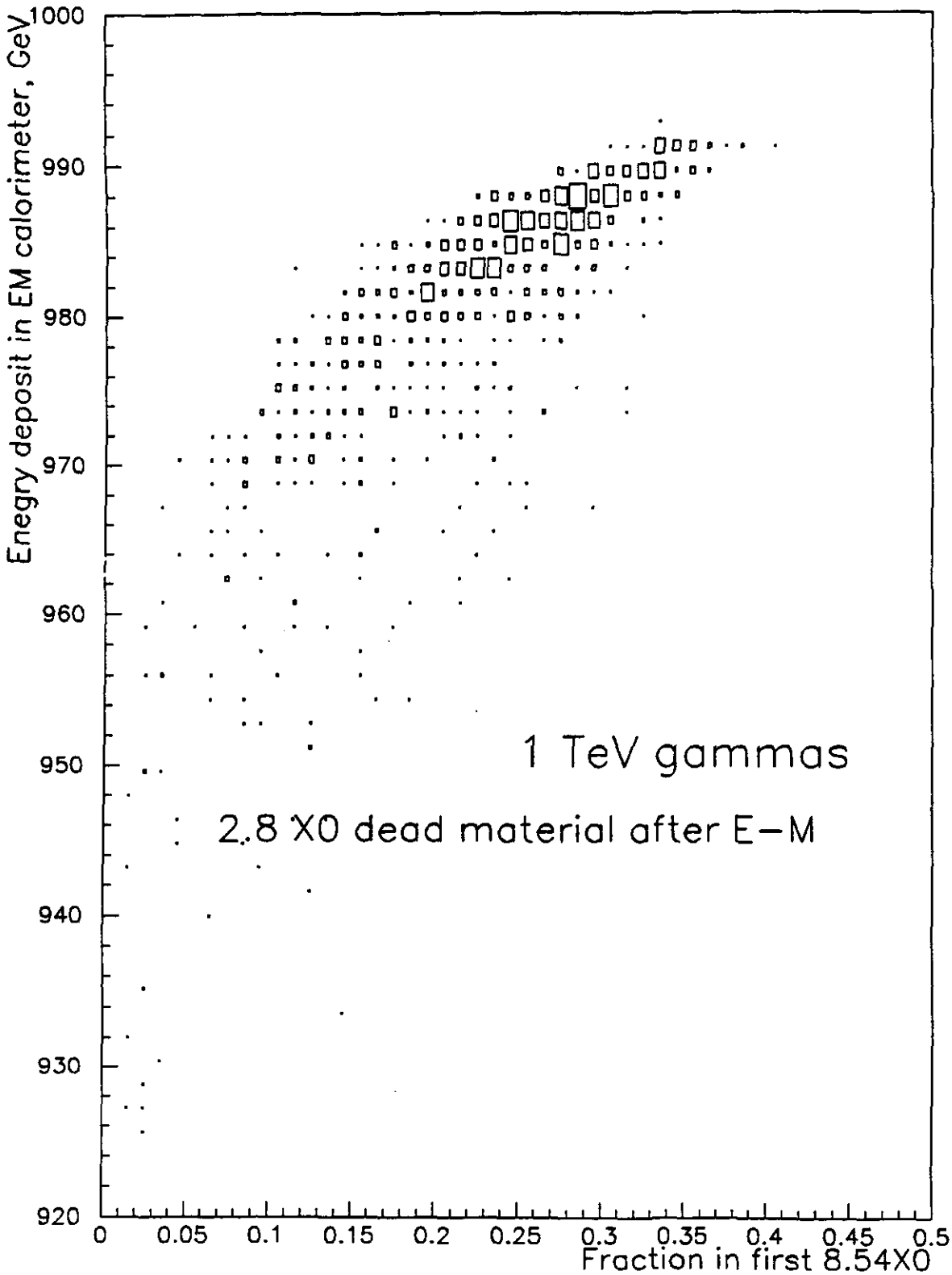

'A.Savin/

Fig IV-5

APPENDIX 2 — ELECTRON - PION DISCRIMINATION (Yu. Efremenko)

In this study a full GEANT3 simulation with a magnetic field 0.8 T.was used. In fig. 1 the three different geometries used are shown:

Baseline -	the so-called Integrated Calorimetry option with the thin (1.4 X0) wall between EM and HCAL section.
Hybrid -	LKr EM and Scintillating Fiber HCAL sections. The only difference is the wall thickness (2.8 X0).
Hybrid 3λ -	LKr EM, 3 interaction length LAr HCAL and Scintillating Fiber HCAL sections.

In Fig 2-3 the energy deposition in HCAL for 100 GeV electrons and pions is shown (Fig.2 is for the Baseline and Fig.3 is for the Hybrid options respectively). Overlapping the electron and pion distributions was used for determining the pion regection factor. The result is shown in Fig 4.

It is seen that for the hybrid option the pion rejection is better than for the Integrated one. The only reason is that the thicker wall works like a tail killer for the EM showers and has negligible influence on the hadronic ones. The rejection for the Hybrid 3λ is the same as for the Baseline option.

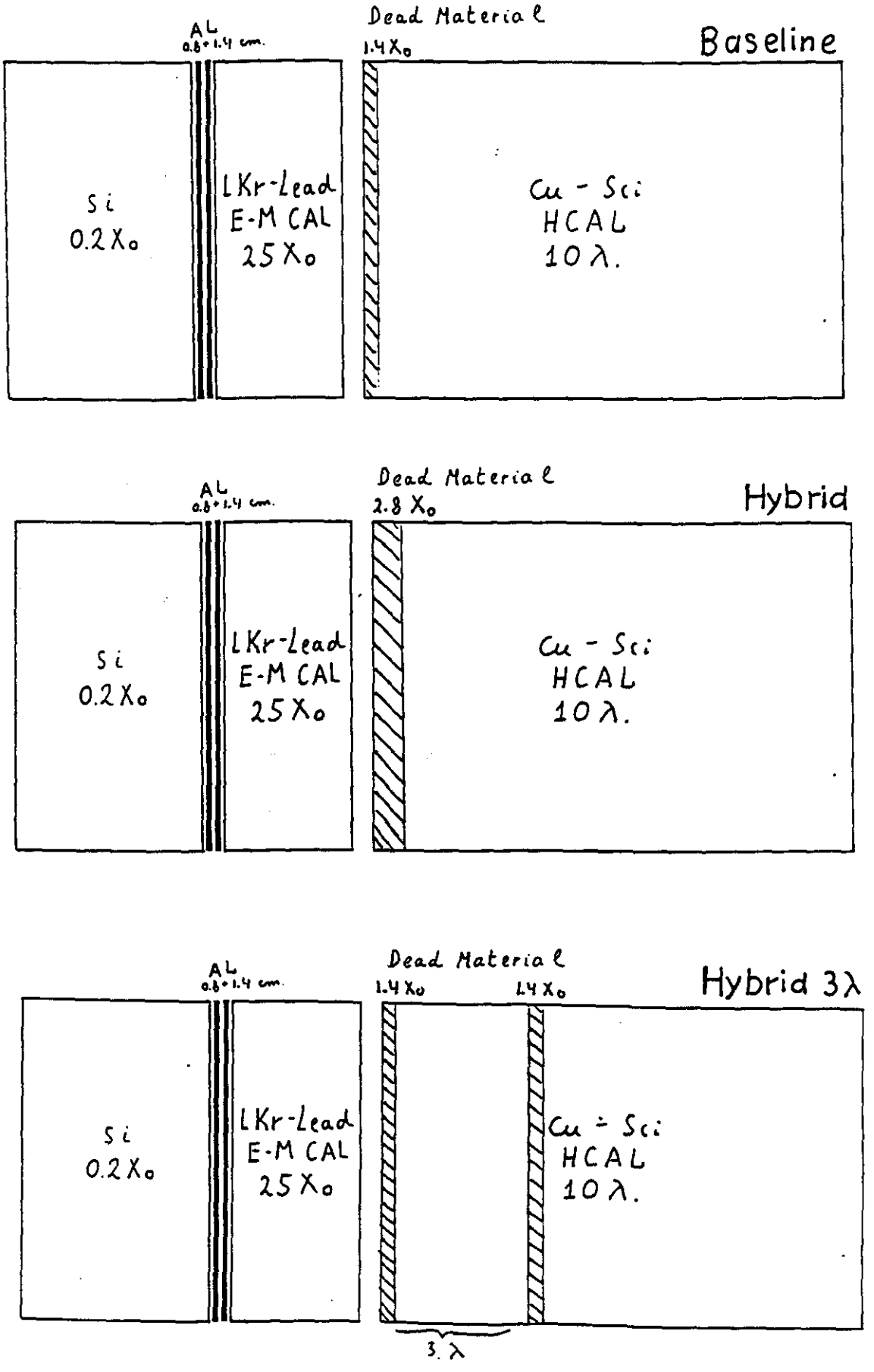
Baseline
Dead Material
1.4 X₀
AL
0.8+1.4 cm.
Si
0.2 X₀
LKr-Lead
E-M CAL
25 X₀
Cu - Sci
HCAL
10 λ.
Hybrid
Dead Material
2.8 X₀
AL
0.8+1.4 cm.
Si
0.2 X₀
LKr-Lead
E-M CAL
25 X₀
Cu - Sci
HCAL
10 λ.
Hybrid 3λ
Dead Material
1.4 X₀
1.4 X₀
AL
0.8+1.4 cm.
Si
0.2 X₀
LKr-Lead
E-M CAL
25 X₀
Cu - Sci
HCAL
10 λ.
3 λ

Fig 1.

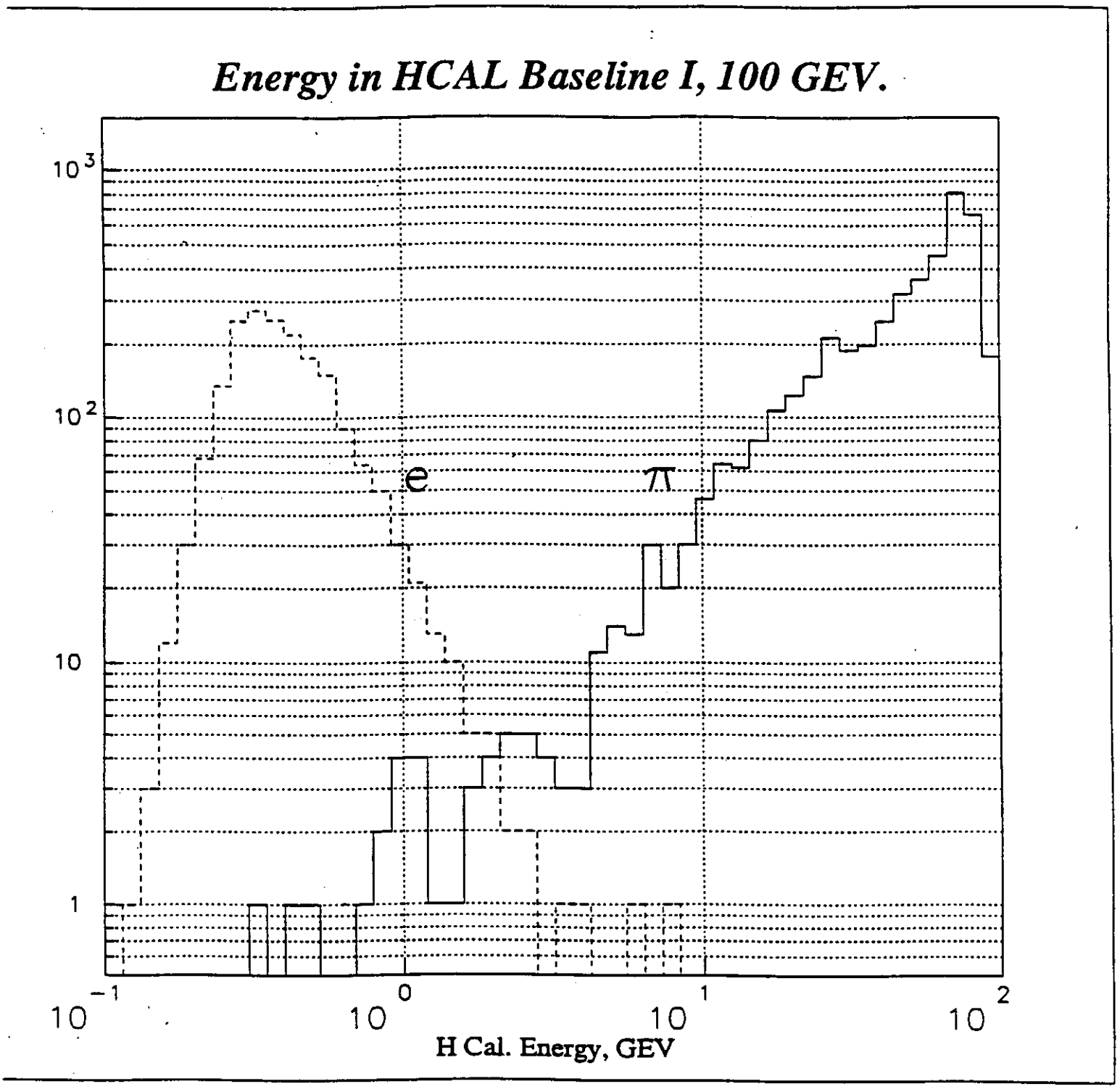
Energy in HCAL Baseline I, 100 GEV.
10^3
10^2
10
1
e
π
10^{-1}
10^0
10^1
10^2
H Cal. Energy, GEV

Fig 2

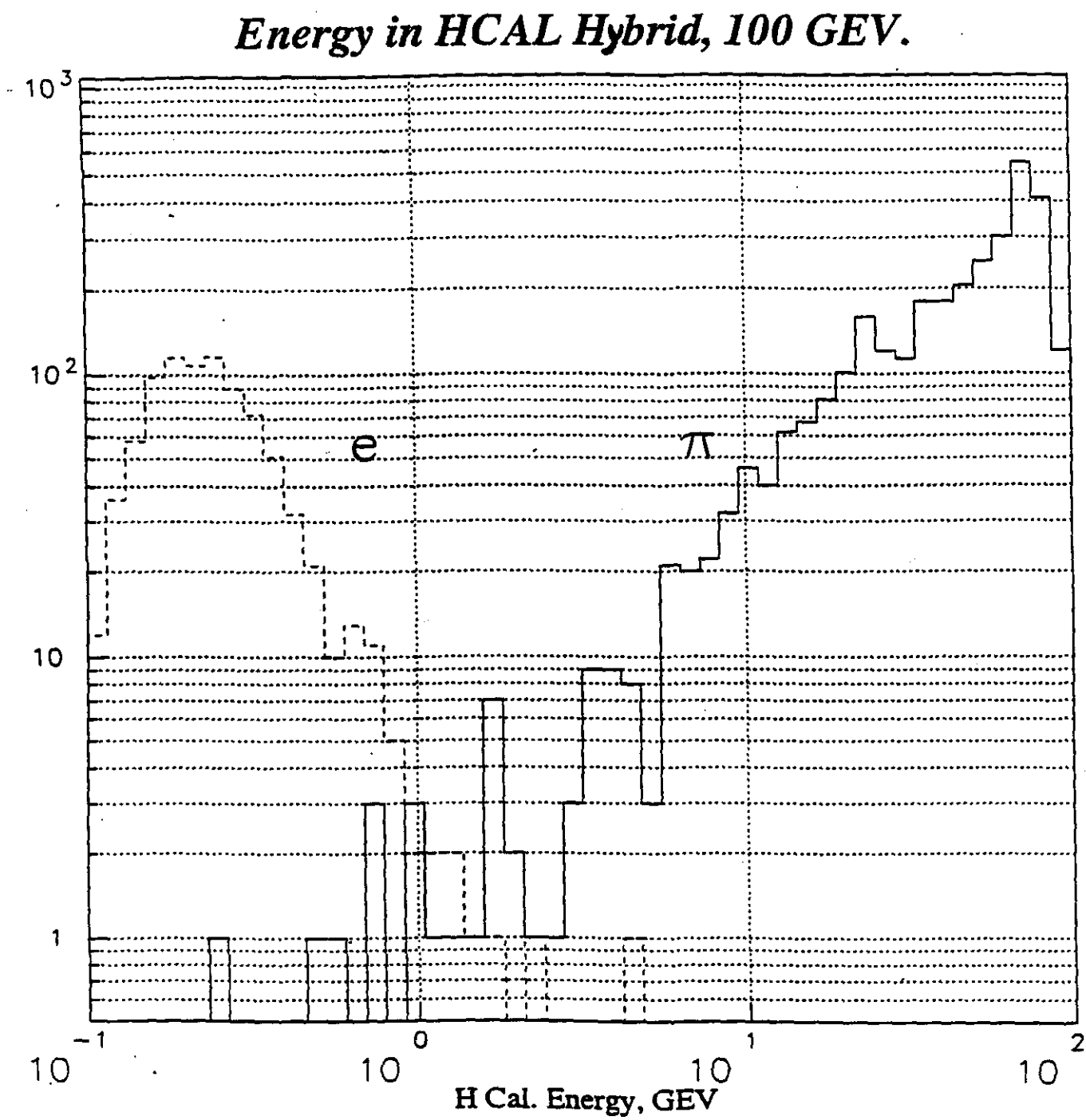
Energy in HCAL Hybrid, 100 GEV.
10^3
10^2
10
1
e
π
10^{-1}
10^0
10^1
10^2
H Cal. Energy, GEV

Fig 3

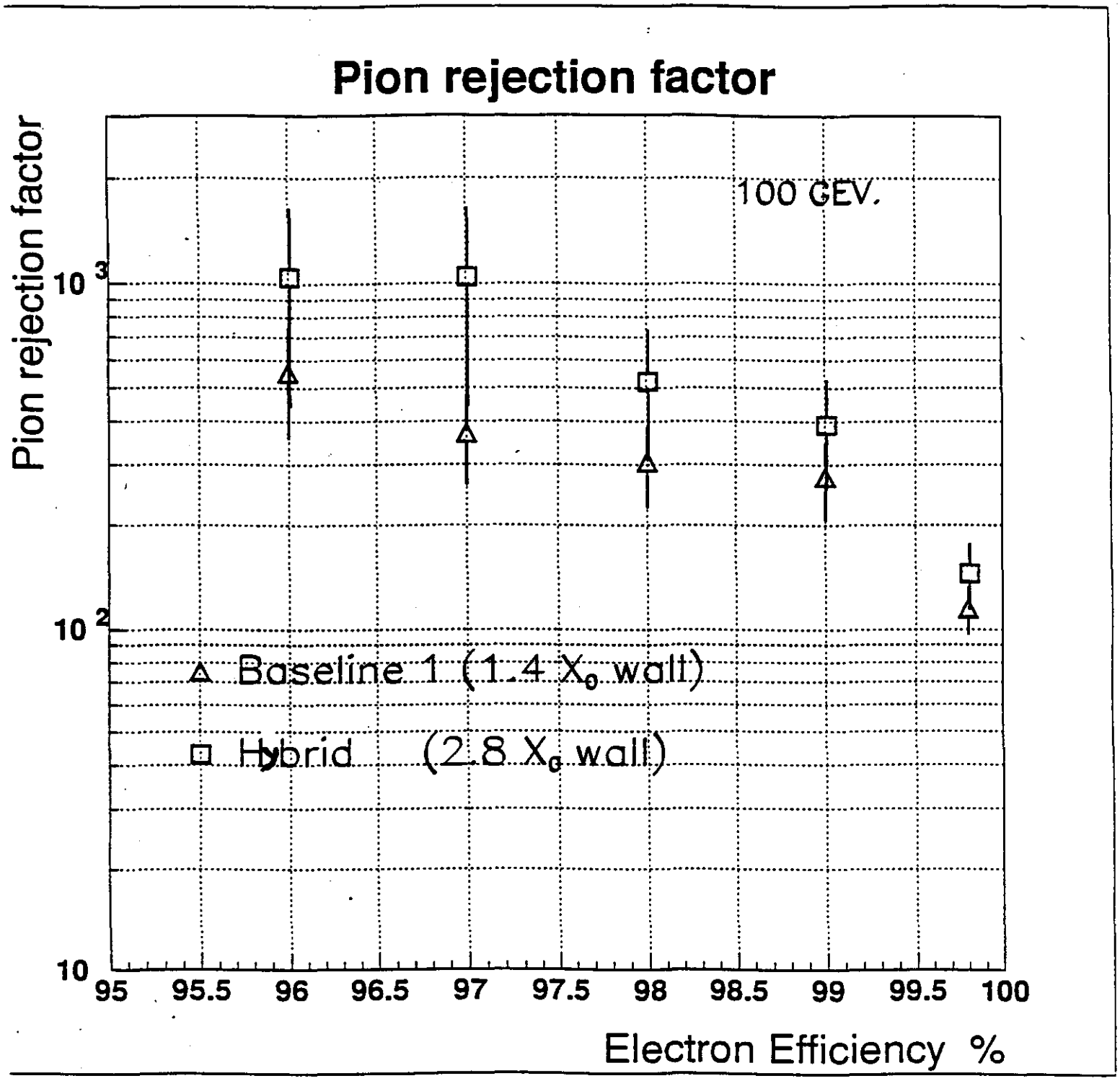
Pion rejection factor
Pion rejection factor
100 GEV.
10^3
10^2
10
Baseline 1 (1.4 X_0 wall)
Hybrid (2.8 X_0 wall)
95
95.5
96
96.5
97
97.5
98
98.5
99
99.5
100
Electron Efficiency %

Fig 4

APPENDIX 3 — MISSING E_T IN CRYOSTAT WALLS (K. Shmakov)

Particles (mainly hadrons) may deposit a significant part of their energy in cryostat walls due to energy loss fluctuations which have nongaussian tails. This effect may disturb missing E_T measurements. One can expect the maximum effect if these walls are placed near the hadronic shower maximum (wall between EM Pb/LKr calorimeter and SPACAL) The impact of missing E_T in cryostat walls for the inclusive missing Et measurements was studied for 3 different setups (see Fig.1):

a) Baseline I (EM LAr + HC LAr),
b) Hybrid with 1 lambda hadronic section (EM LKr + 1lambda HC LKr + Scint.HC)
c) Hybrid (EM LKr + Scint.HC)

The following procedure was used:

1) PYTHIA was used to generate about 10K TWOJET events in different P_T ranges from 1-5000 GeV: 1-30 GeV, 30-80 GeV, 80-150 GeV, 150-300 GeV,...,2000-5000 GeV.

2) GEANT3 was used to generate 1K individual hadrons (π^-) with energies: 1, 2, 3, 4, 5, 10, 20, 50, 100, 200, 500GeV. Setups a),b),c) (Fig.1) at 90 deg. were used with various thicknesses of cryostat walls (Al) after the EM calorimeter and after 1 lambda HC section. Energy depositions in cryostat walls were measured for each set of parameters (energy and thickness).

3) The tails of the above distributions of energy loss in cryostat walls were fitted by an exponential function:

$$y = p1*\exp(p1+E*p2)$$

- Parameter p2 reflects the tail decrease,
- ratio exp(p1)/p2 reflects the number of events in a tail over the total number of events - the probability to be in a tail.

Examples of such distributions with corresponding fits are shown in Fig.2-7 for 10,50 and 500 GeV.

Both parameters - tail decrease and probability to be in a tail - were fitted and parametrized in 3 dimensions independently:

- for a fixed wall thickness but variable energy,
- for a fixed energy but variable wall thickness.
- the transition between wall after EM calorimeter and wall after additional Hadronic section for a fixed wall thickness and energy.

This parametrization gives the parameters of the tail for energy loss in a wall for arbitrary energy and thickness. Using these parameters later one can calculate the probability of the specific energy loss of a hadron at arbitrary theta angle in a cryostat wall. An example of such parametrization is shown in Fig.8.

Finally, using (1) for all TWOJET envents the energy loss of hadrons was randomely chosen (from the parametrizations) and the total missing E_T was calculated. In addition the missing E_T due to neutrinos only was calculated for the same events.

In the paper of Frank.E.Paige and A.V.Vanyashin (GEM TN-92-70) it was shown that neutrinos can carry out significant E_T and this E_T represents the irreducible background (Fig.9). It was also shown that the effect of limited calorimeter coverage gives an additional huge rate for missing E_T in the range $E_T < 100$ GeV due to jet leakages in the forward region. This makes impossible any E_T measurements below

100GeV. From the above one can conclude that any additional missing E_T effects should be compared with the irreducible missing E_T above 100 GeV from neutrinos.

This is done in Fig.10,11,and 12 for setups a),b) and c) respectively. It is obvious that for all setups the effect of additional missing E_T is far below the irreducible background from neutrinos. The comparison of all 3 setups is given in Fig.13. If one compares the total availabe E_T in a jet with the missing E_T in the walls one can see (Fig.14) that the latter is much less; this is the effect of randomisation of energy loss from all hadrons.

It is esential to note that the consideration above includes energy loss in the dead material inside the hadronic shower without any corrections. For the real SSC events in GEM with any of the proposed configurations one can in principle correct for the average energy loss in the dead material by appropriate calibration of the combined EM+Hadron system and correct for fluctuations of energy loss in dead material by looking at the correlation between energy deposited in EM and Hadronic sections. This should reduce significantly the missing E_T.

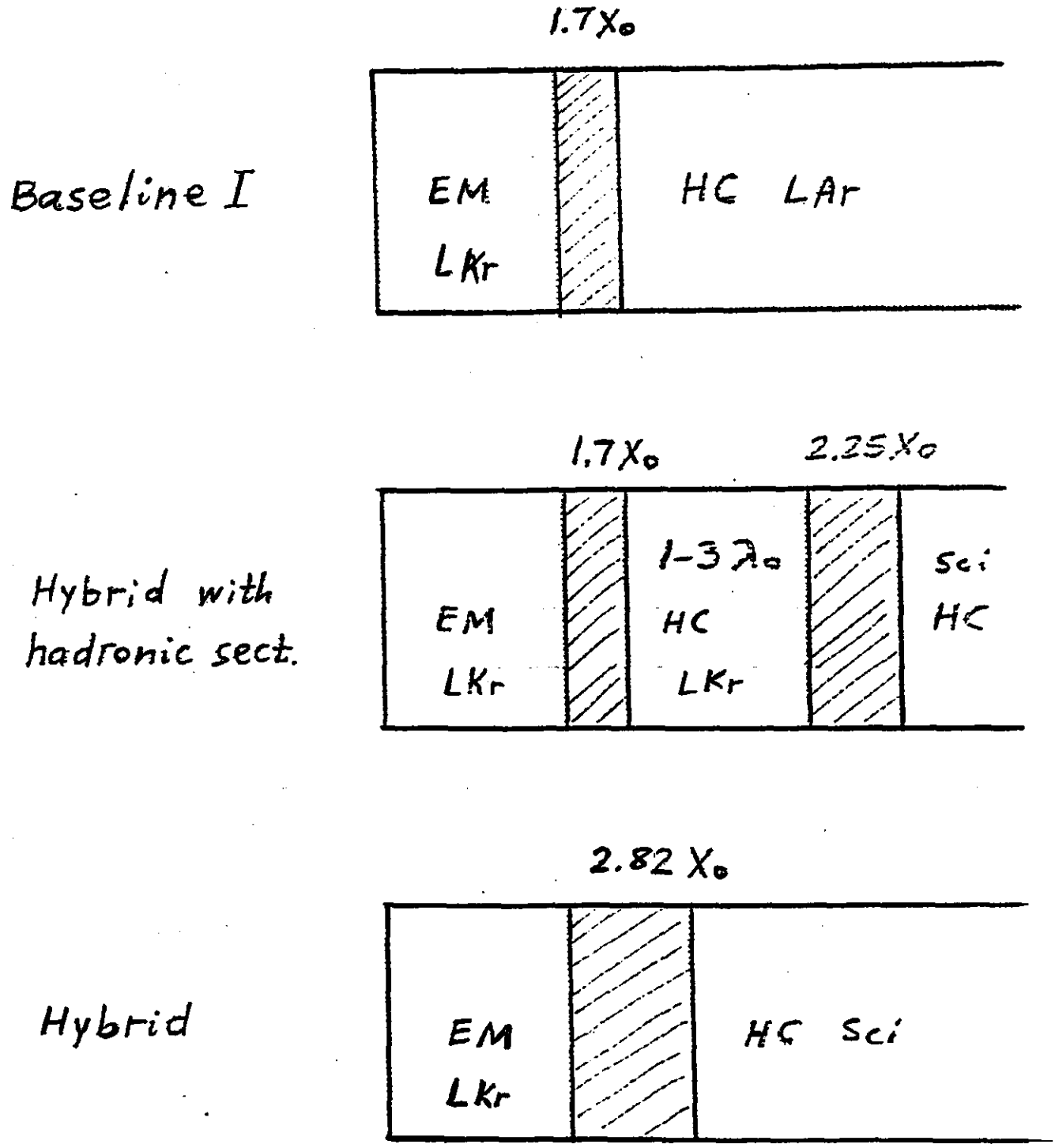

Dead material between E-M and hadronic sections

Fig. 1

10 GeV pions-

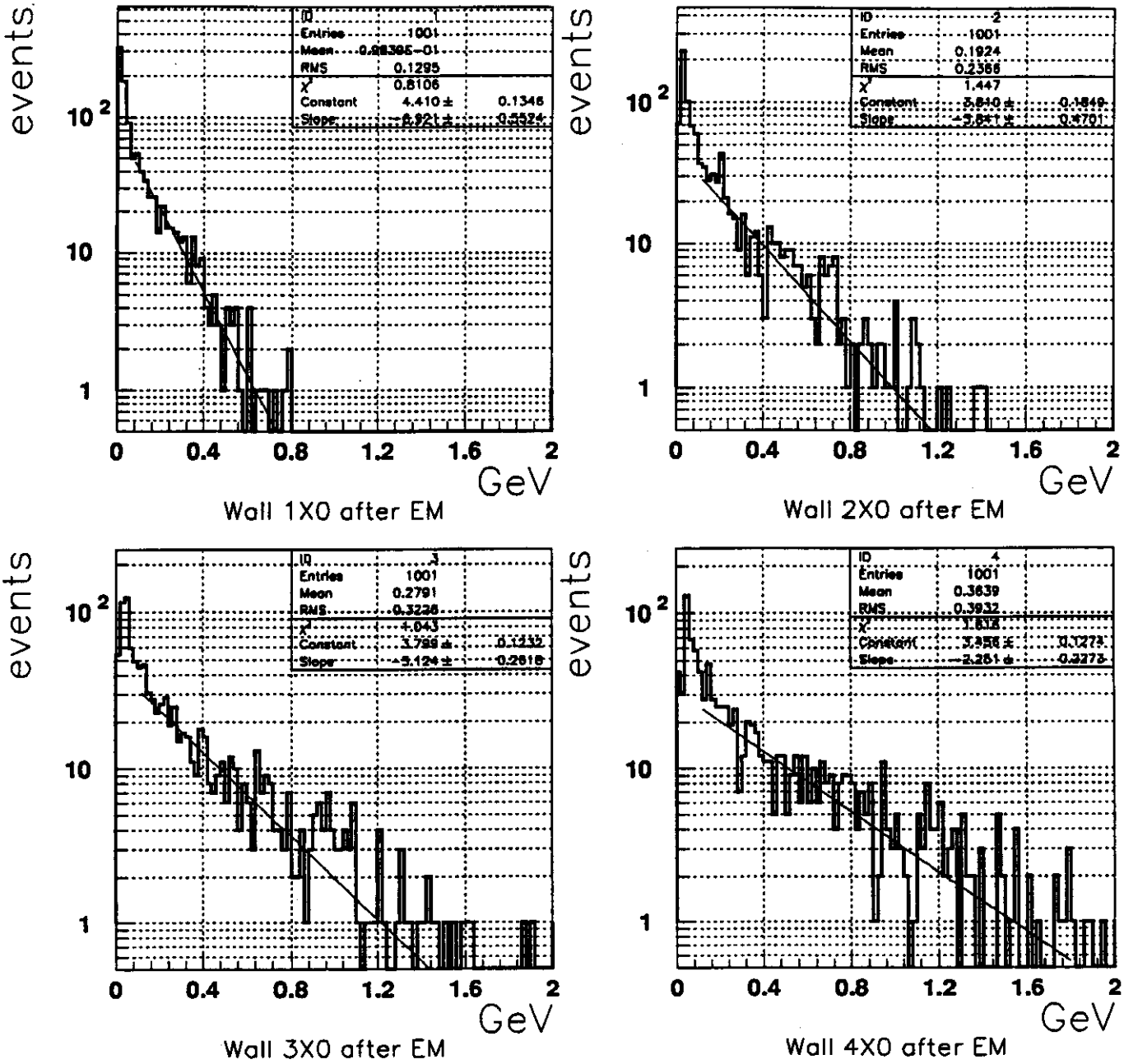

Fig. 2

10 GeV pions-

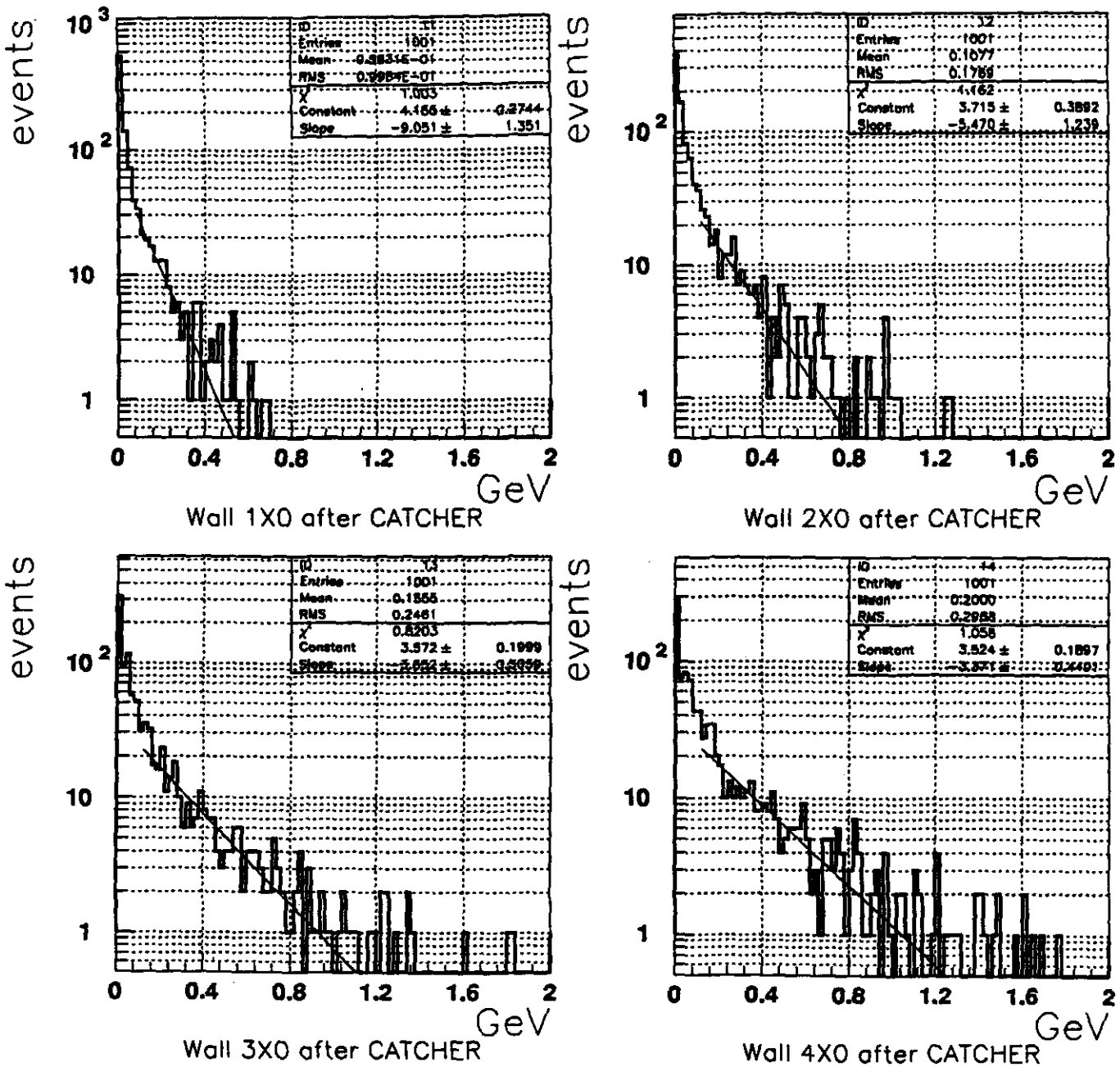

Fig. 3

50 GeV pions-

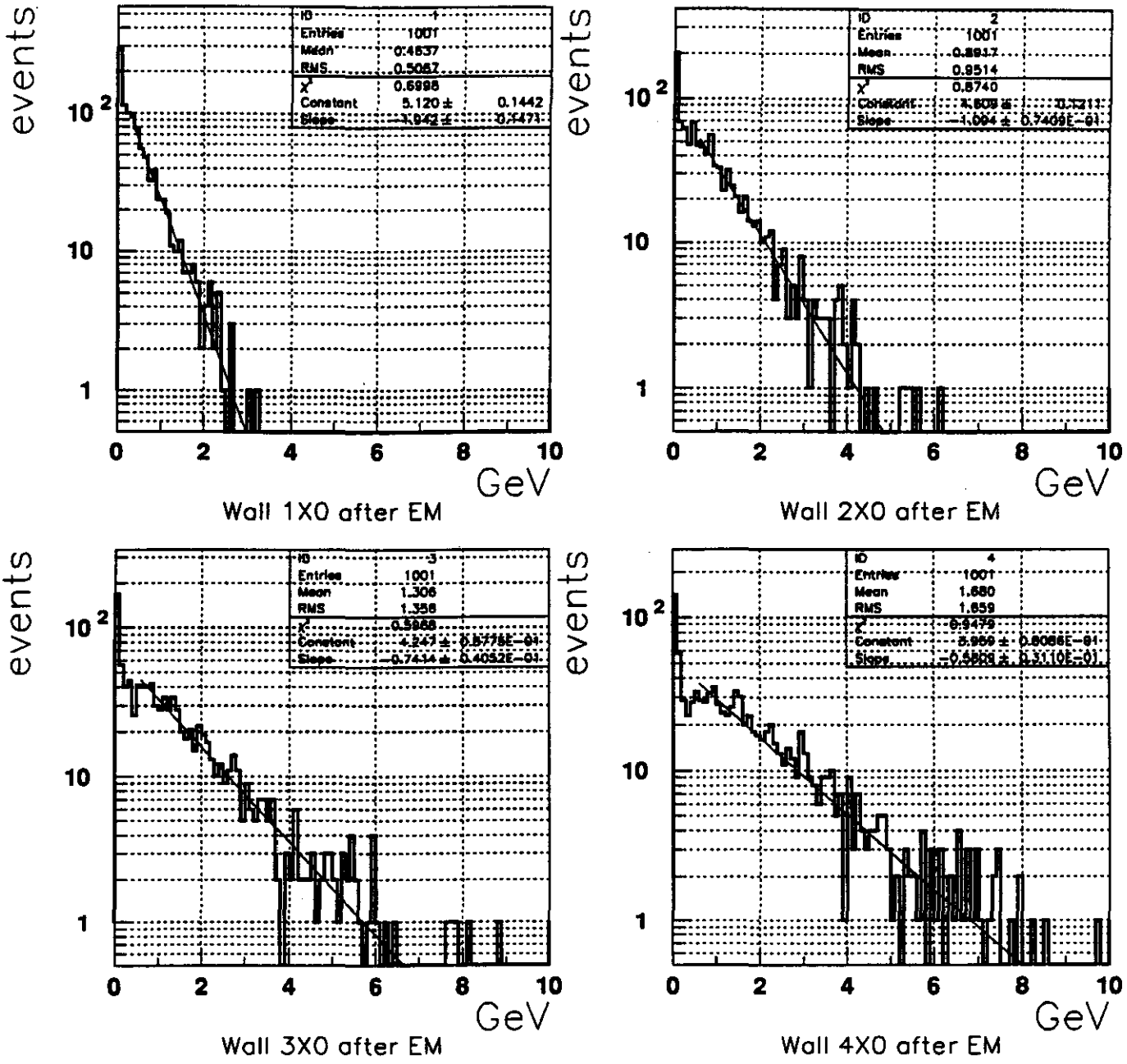

Fig. 4

50 GeV pions-

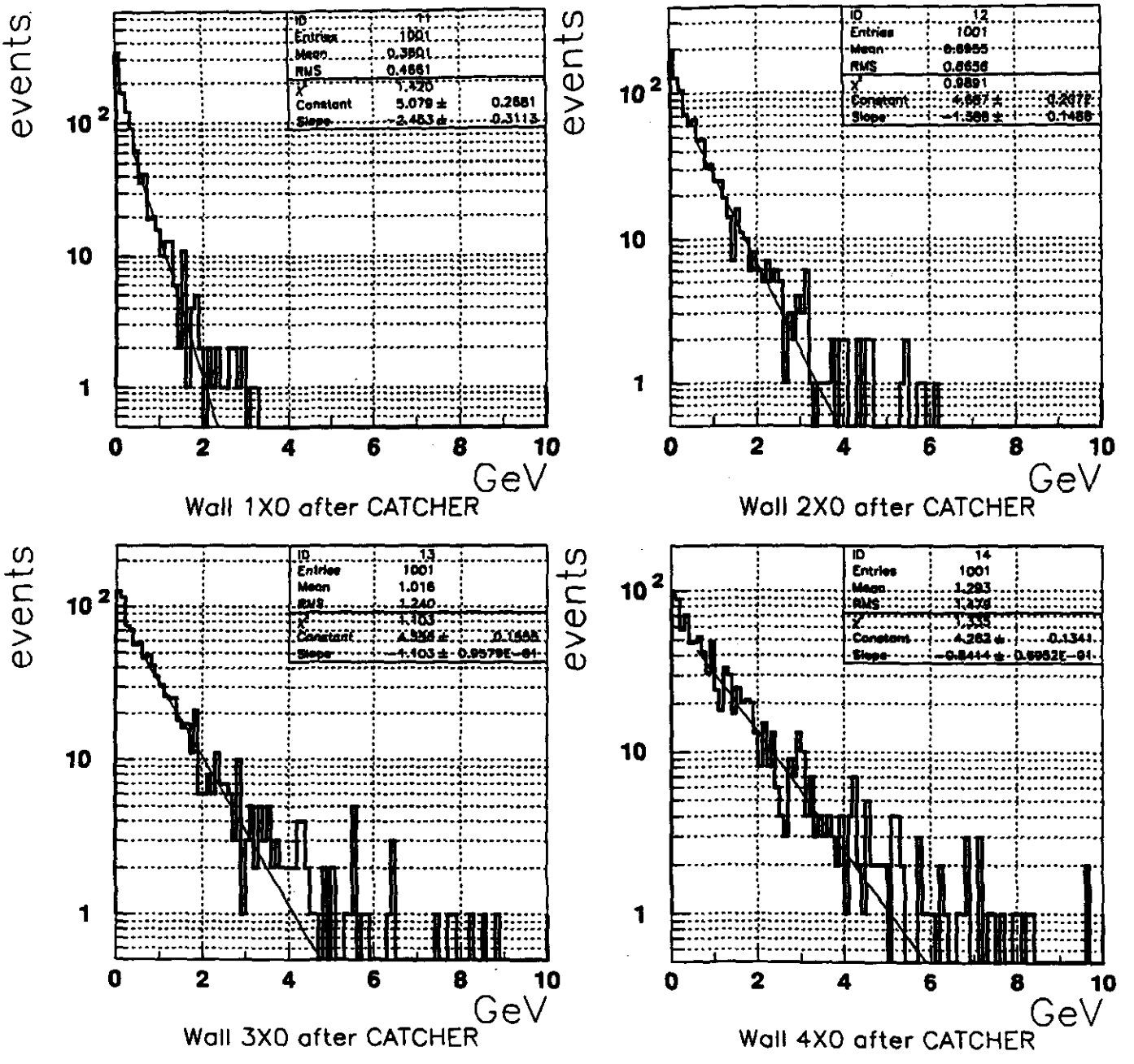

Fig. 5

500 GeV pions-

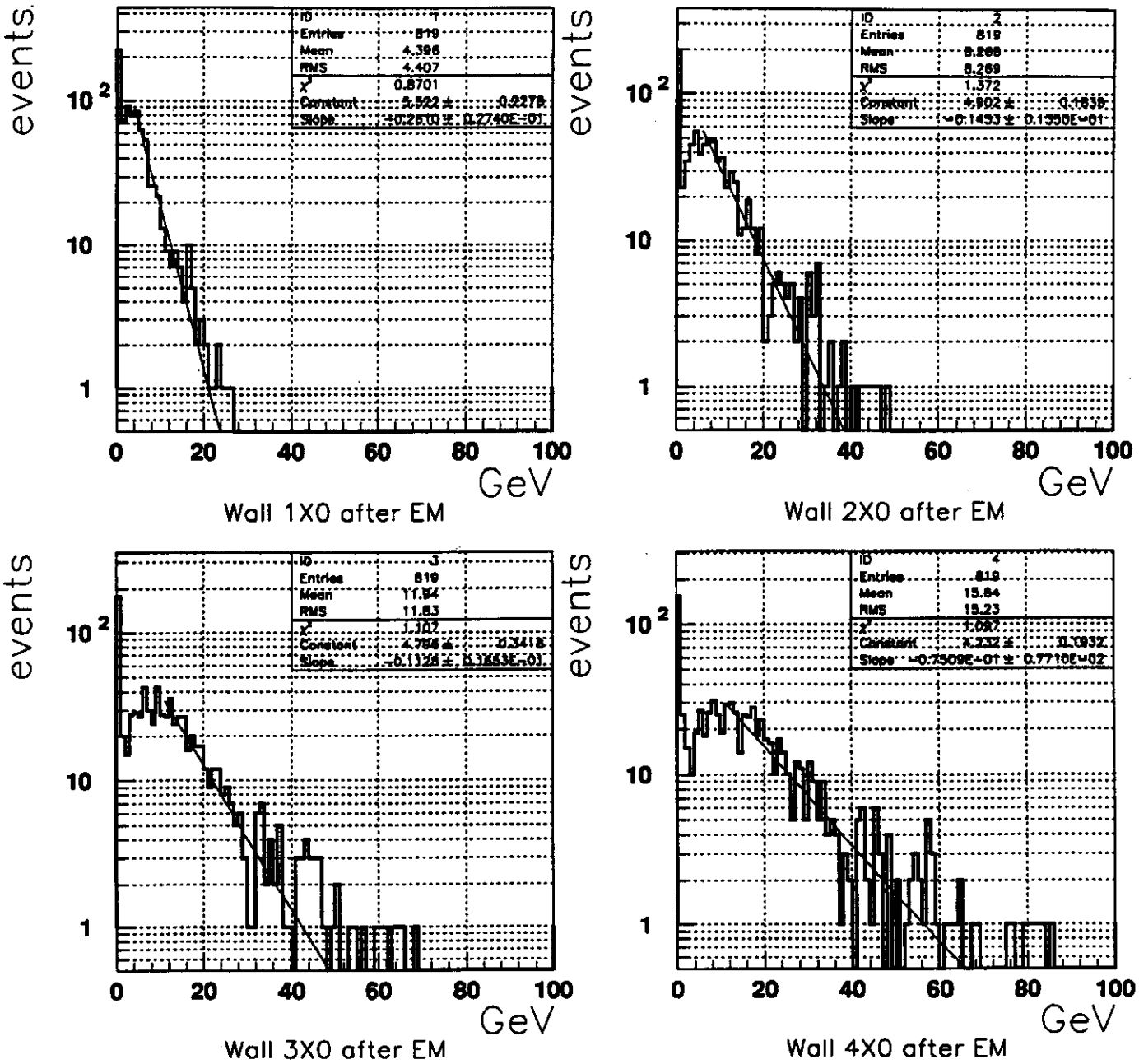

Fig. 6.

500 GeV pions-

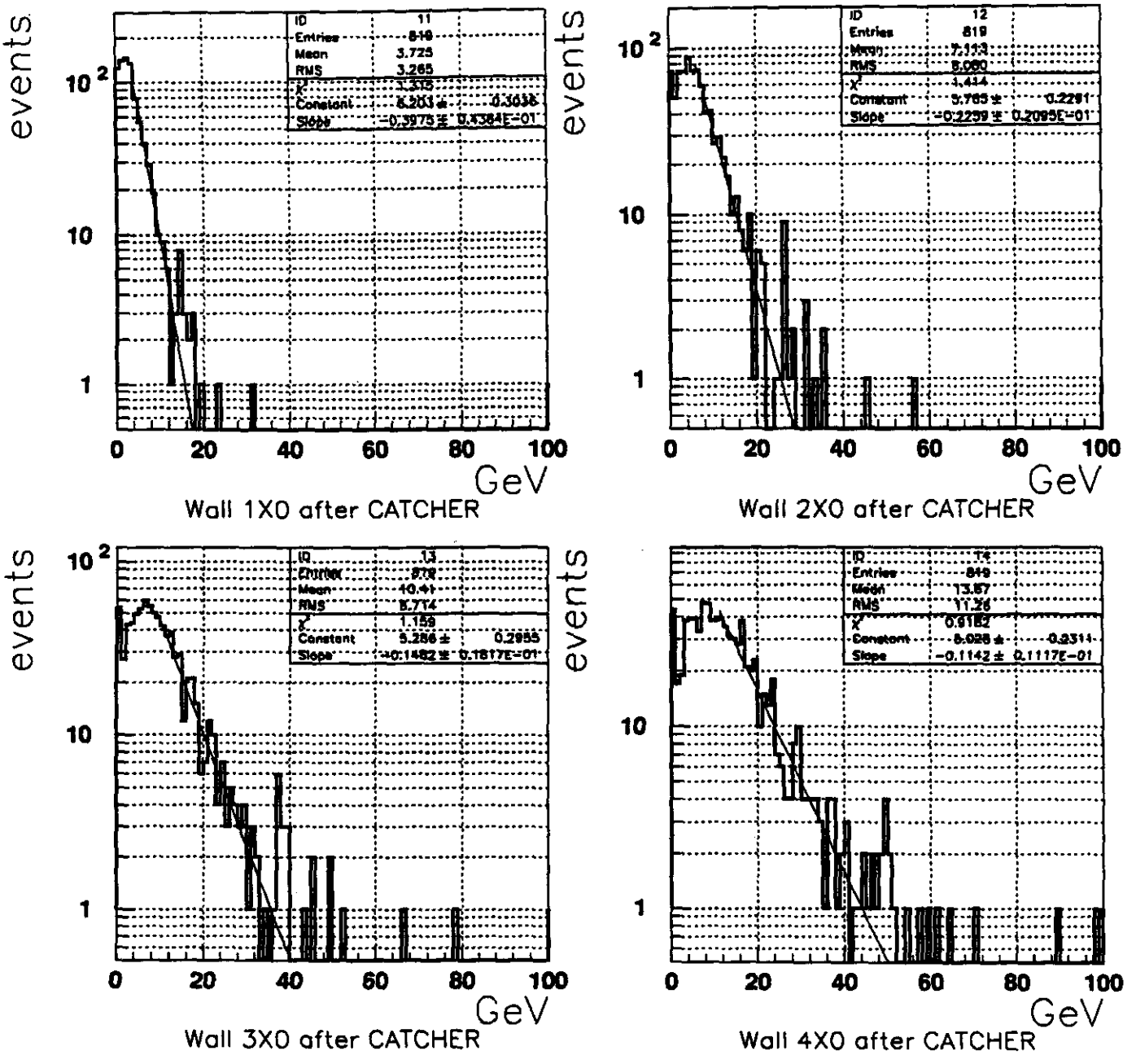

Fig. 7

Parametrisation of the pi- energy loss in dif. (cryostat) walls

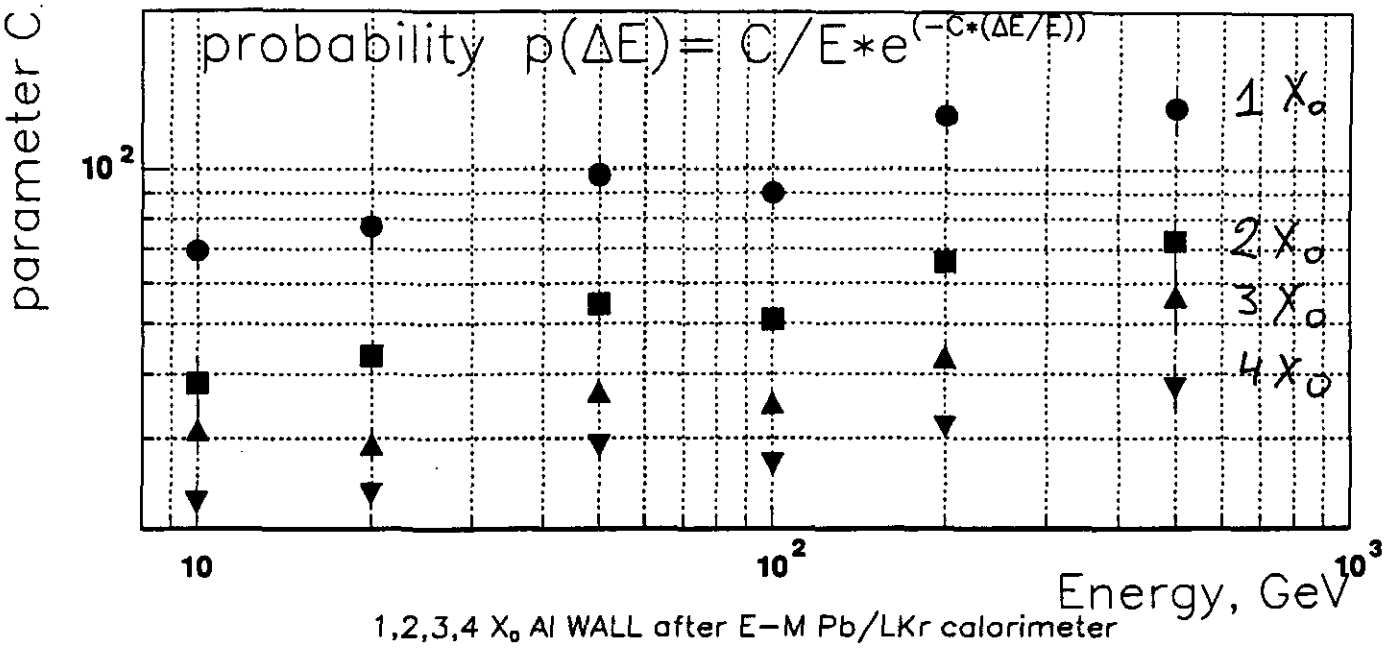

1,2,3,4 X_0 Al WALL after E−M Pb/LKr calorimeter

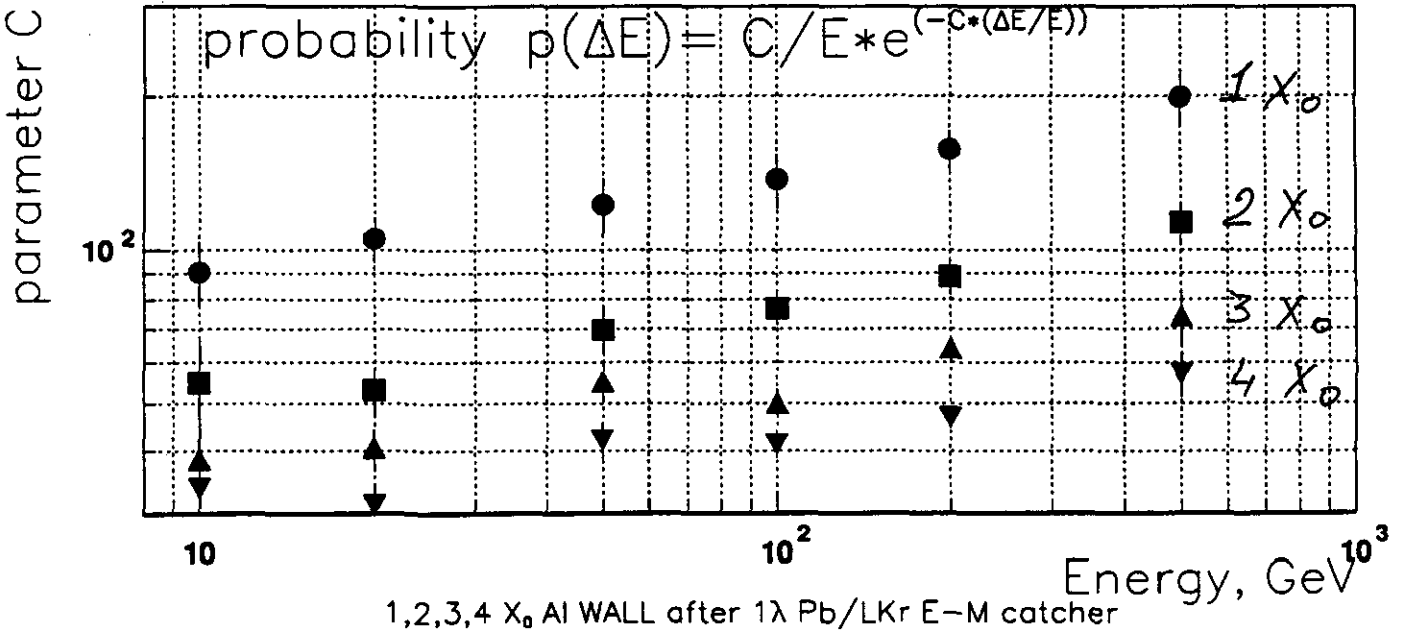

1,2,3,4 X_0 Al WALL after 1λ Pb/LKr E−M catcher

Fig. 8

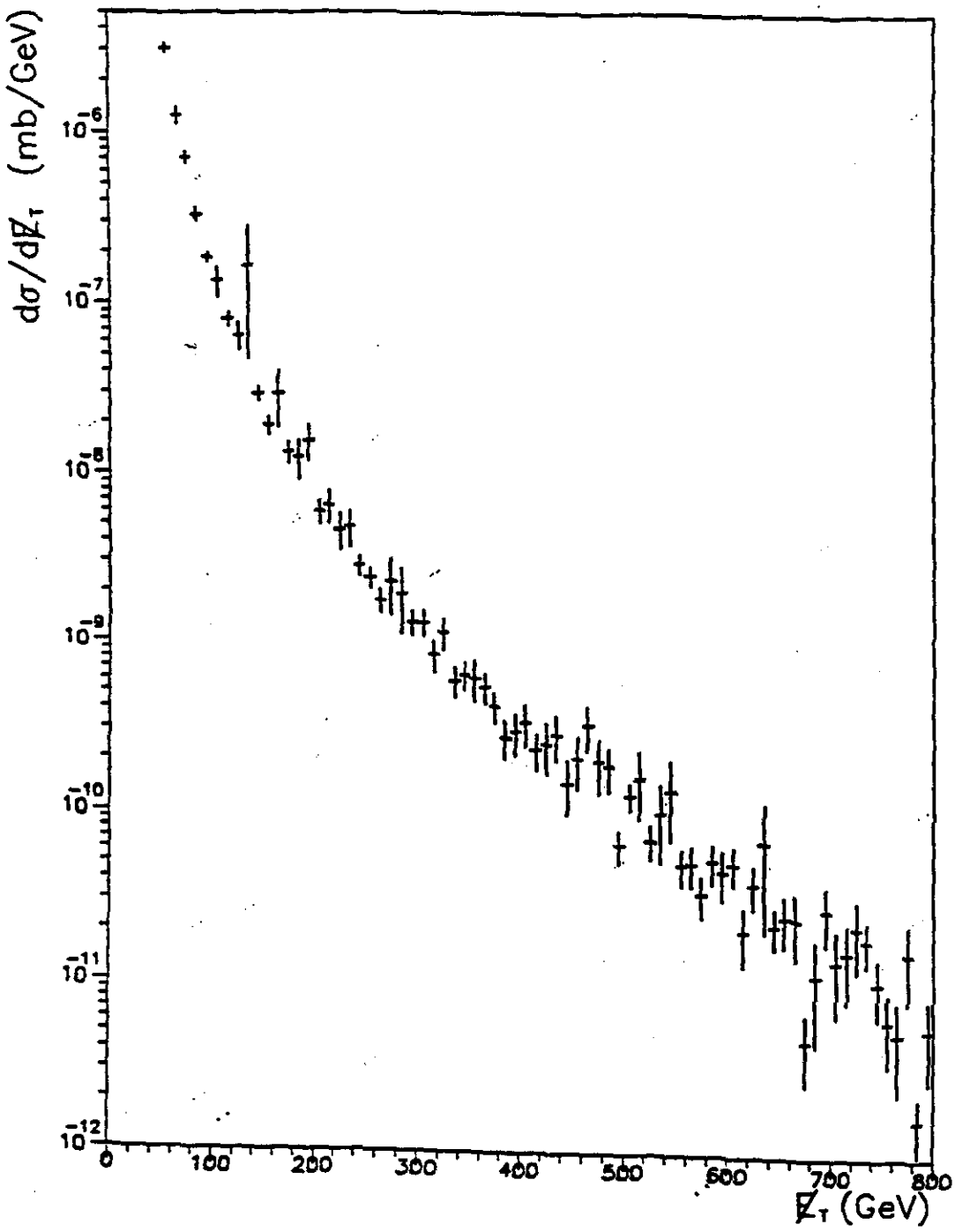

Figure 2.1: True $\not{E}_T$ cross section from neutrinos from heavy quark decays.

Fig. 9

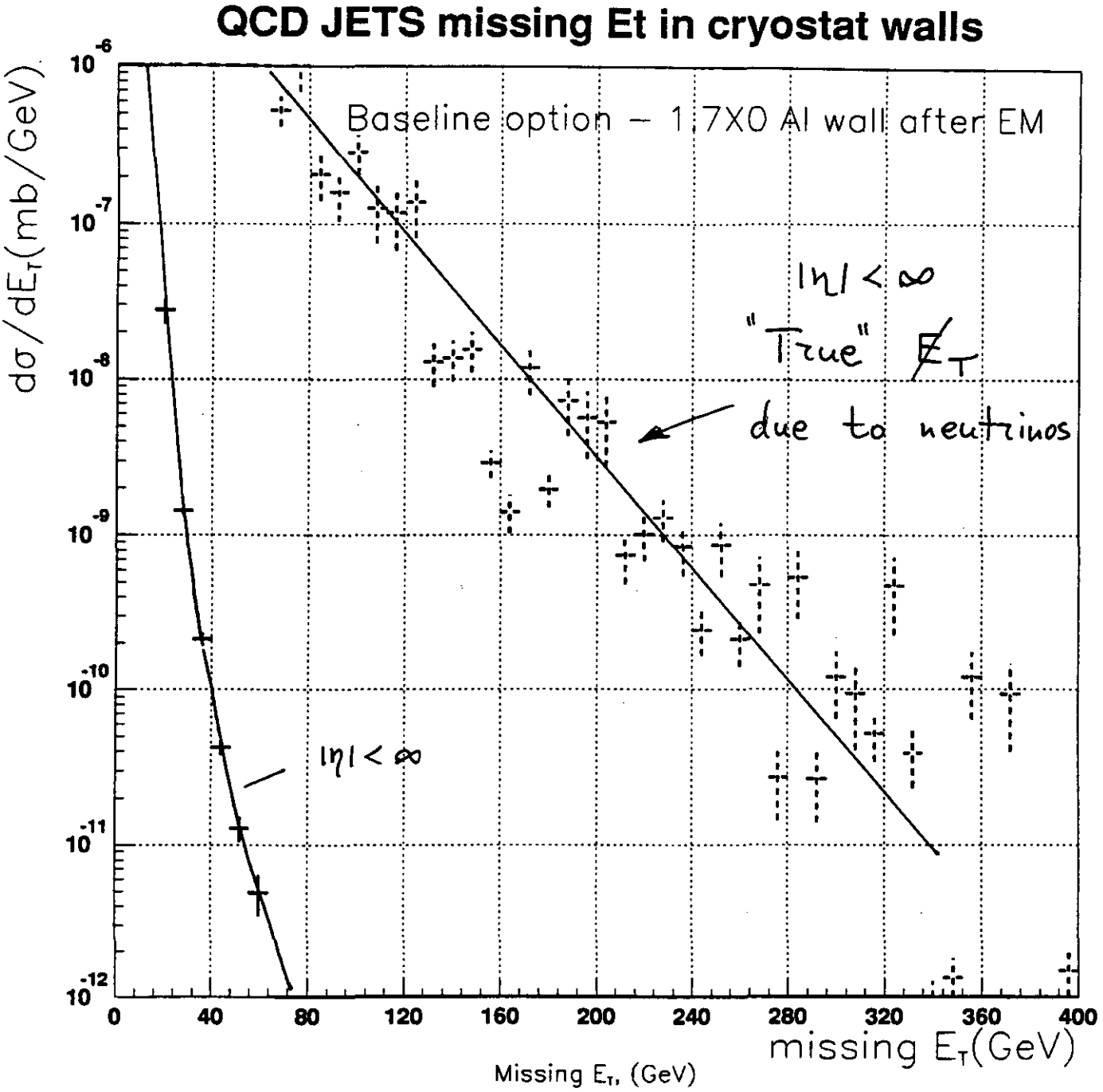
QCD JETS missing Et in cryostat walls
Baseline option – 1.7X0 Al wall after EM
dσ/dE_T(mb/GeV)
|η| < ∞
"True" E̸_T
due to neutrinos
|η| < ∞
missing E_T(GeV)
Missing E_T, (GeV)

Fig. 10

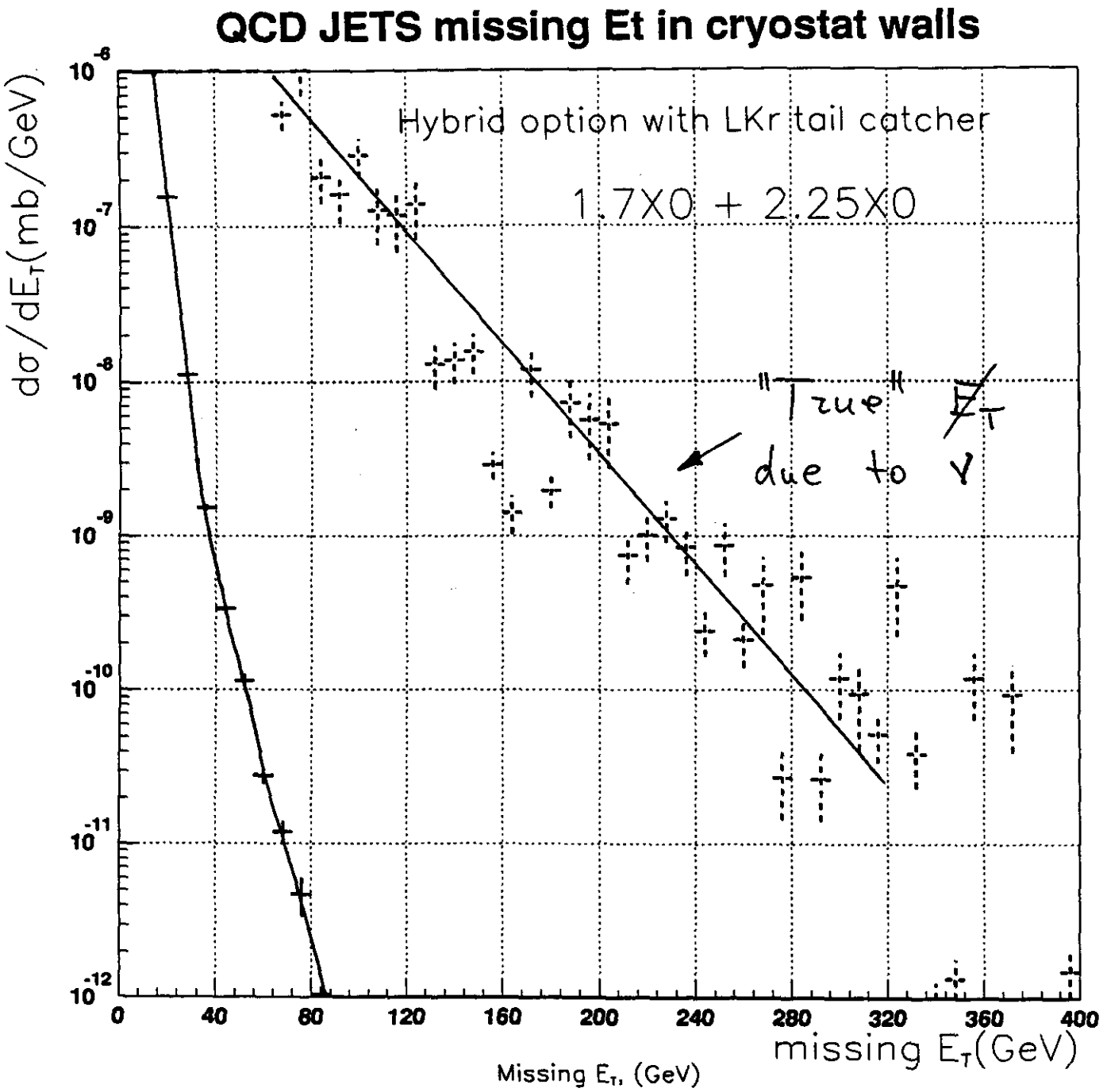
QCD JETS missing Et in cryostat walls
Hybrid option with LKr tail catcher
1.7X0 + 2.25X0
"True" $\not{E}_T$
due to ν
$d\sigma/dE_T$(mb/GeV)
missing E_T(GeV)
Missing E_T, (GeV)

Fig. 11

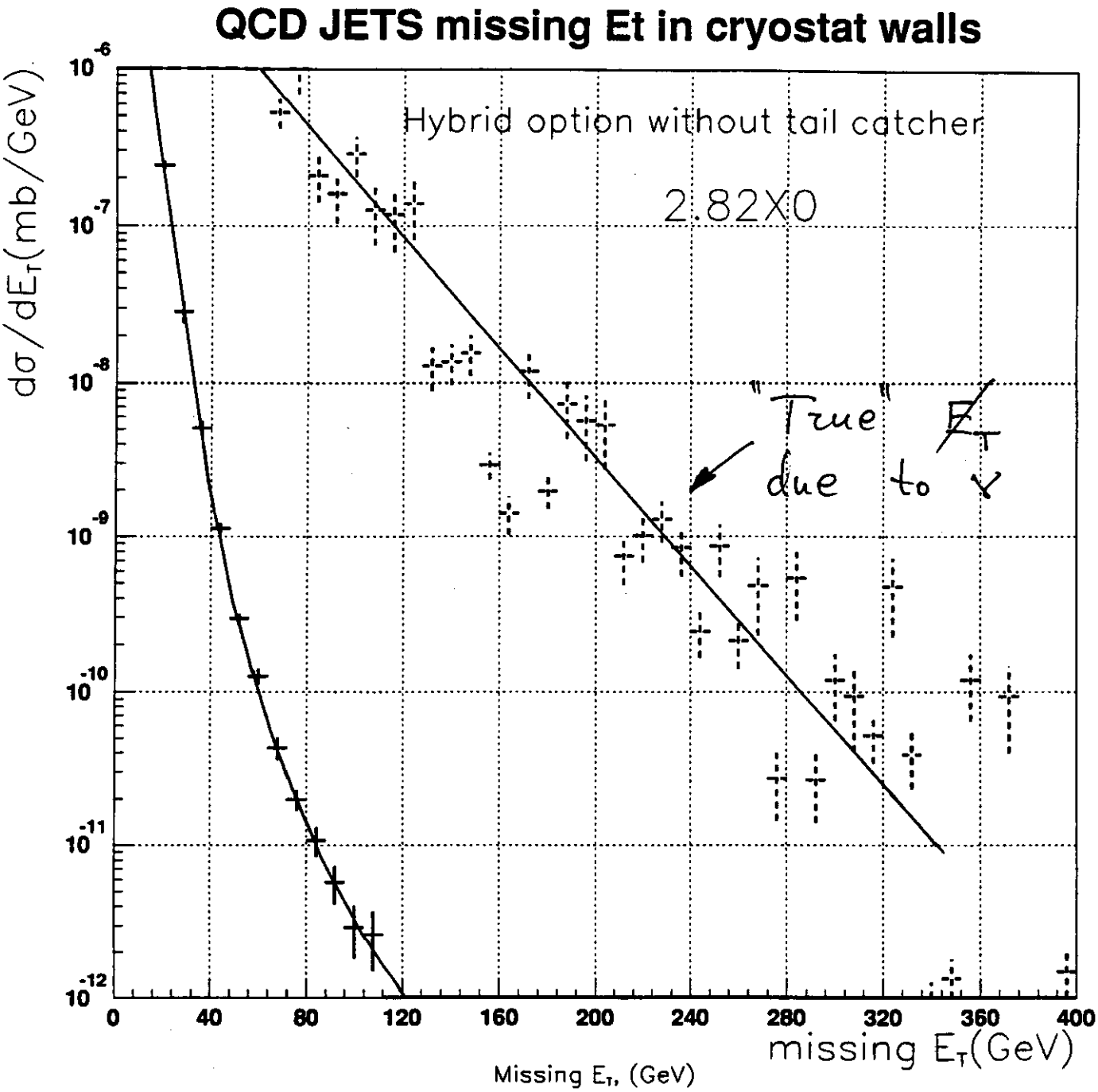
QCD JETS missing Et in cryostat walls
Hybrid option without tail catcher
2.82X0
"True" $\not{E}_T$ due to ν
$d\sigma/dE_T$(mb/GeV)
missing E_T(GeV)
Missing E_T, (GeV)

Fig. 12

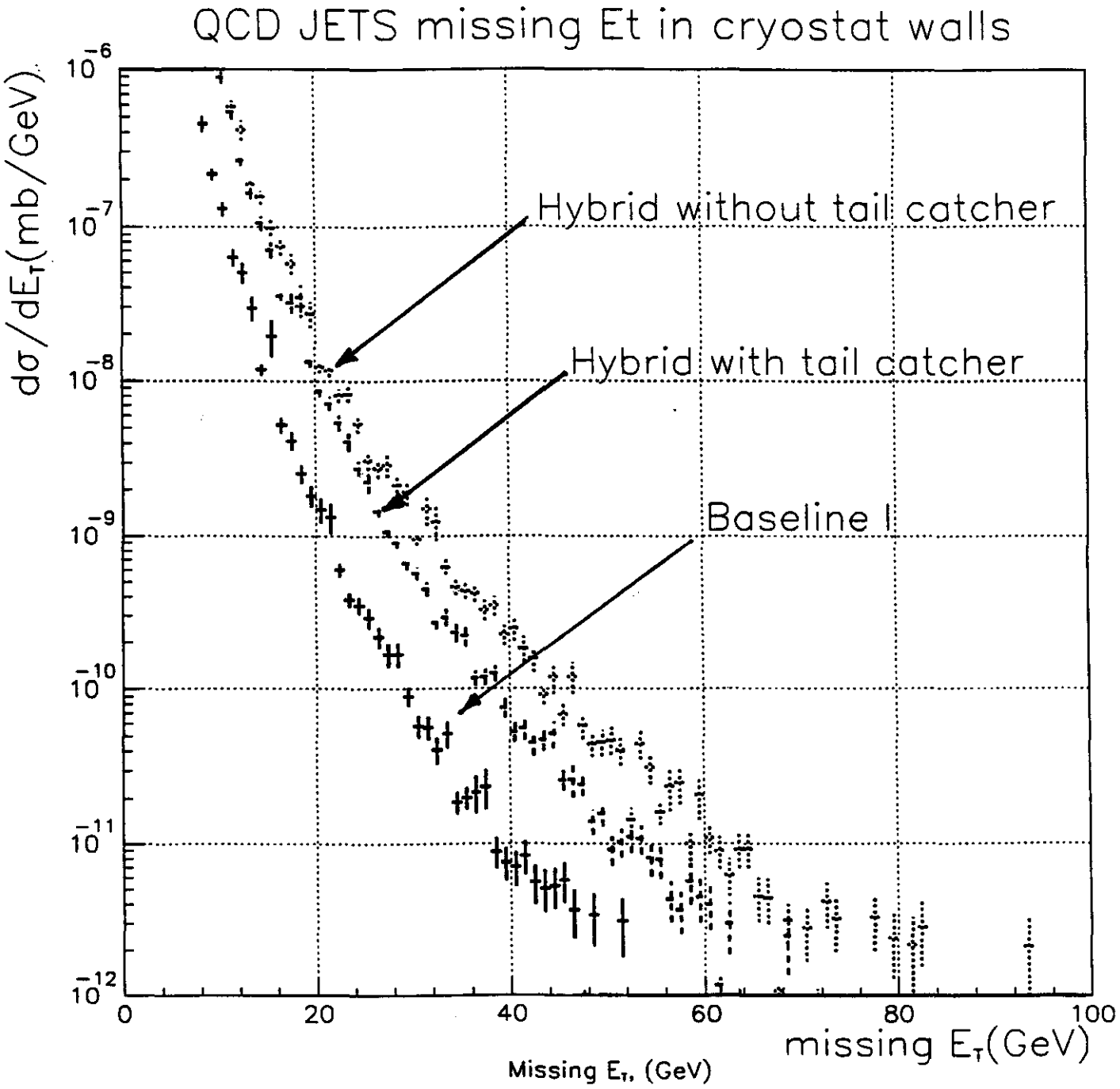
QCD JETS missing Et in cryostat walls
dσ/dE_T(mb/GeV)
Hybrid without tail catcher
Hybrid with tail catcher
Baseline I
missing E_T(GeV)
Missing E_T, (GeV)

Fig. 13

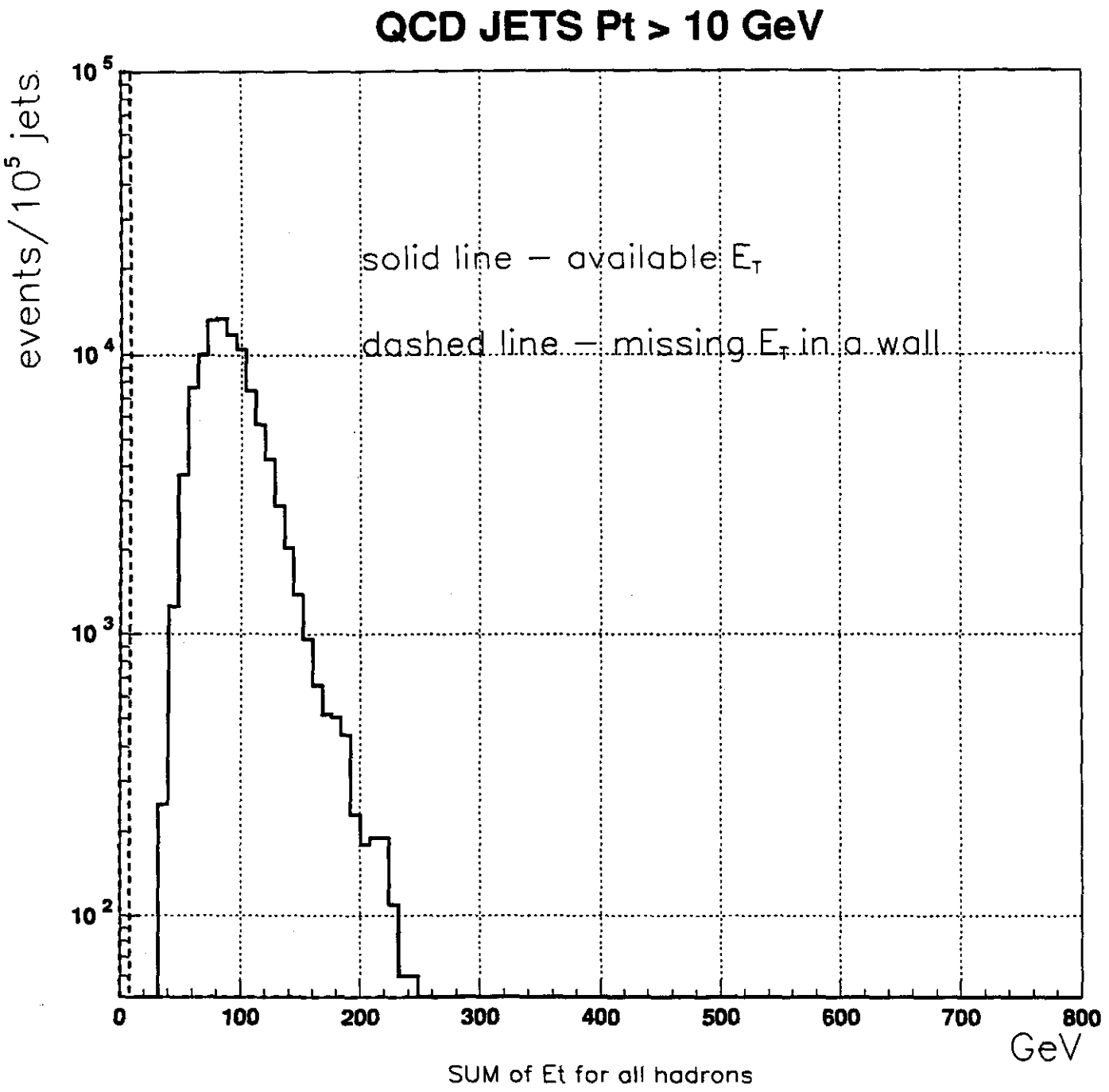
QCD JETS Pt > 10 GeV
events/10^5 jets
10^5
10^4
10^3
10^2
solid line – available E_T
dashed line – missing E_T in a wall
0
100
200
300
400
500
600
700
800
GeV
SUM of Et for all hadrons

Fig. 14

APPENDIX 4 — HADRONIC RESOLUTION (Yu. Efremenko)

The geometries used are the same as those shown in Appendix 2, Fig 1. In Fig 5,6, and 7, 100 GeV pion energy distributions for the three options are shown. For all options the information from the different sections was weighted to achieve the best resolution. It is seen that there is no big difference between the 3 options.

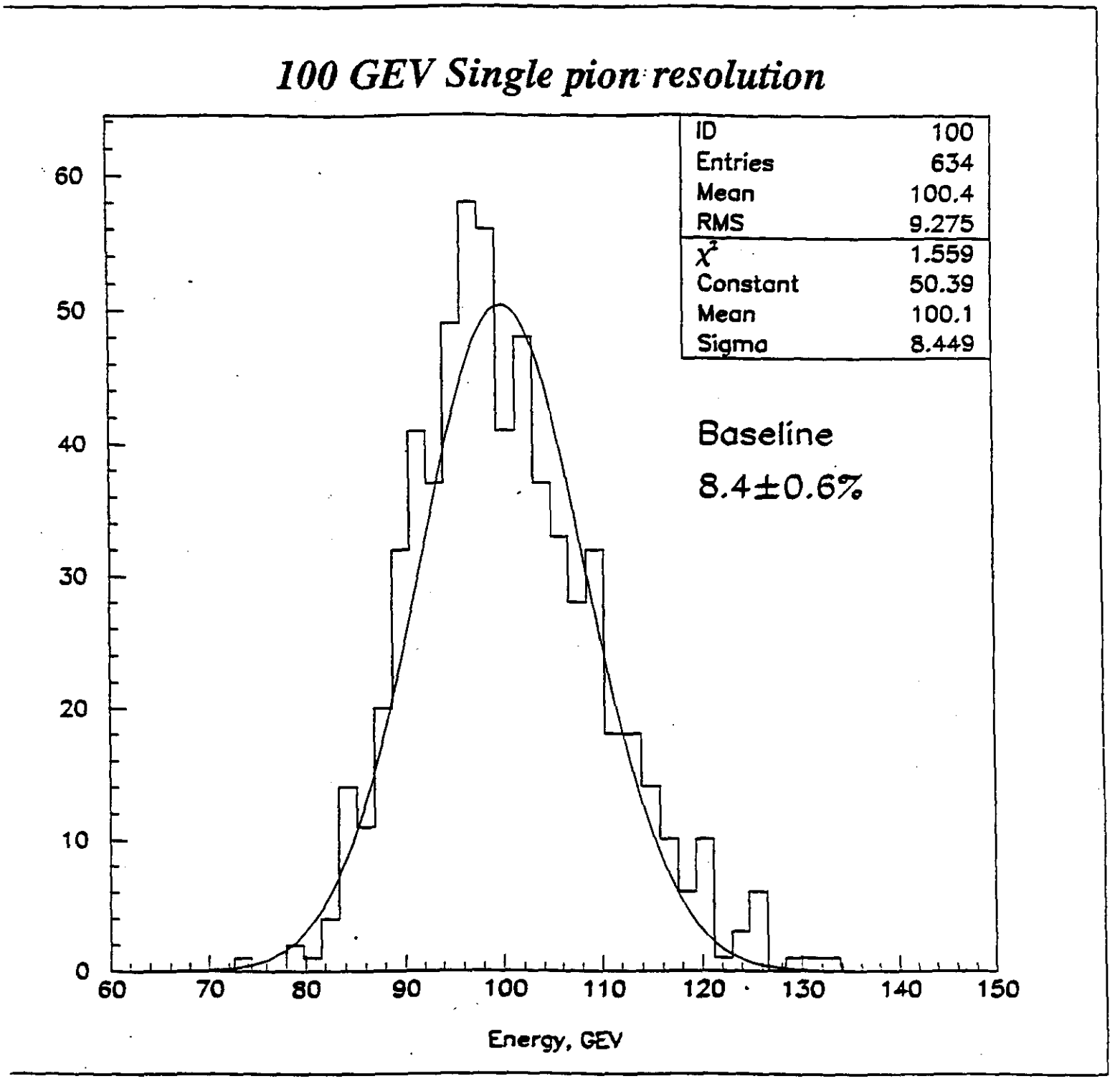
100 GEV Single pion resolution
ID 100
Entries 634
Mean 100.4
RMS 9.275
χ^2 1.559
Constant 50.39
Mean 100.1
Sigma 8.449
Baseline
8.4±0.6%
0
10
20
30
40
50
60
60
70
80
90
100
110
120
130
140
150
Energy, GEV

Fig 5

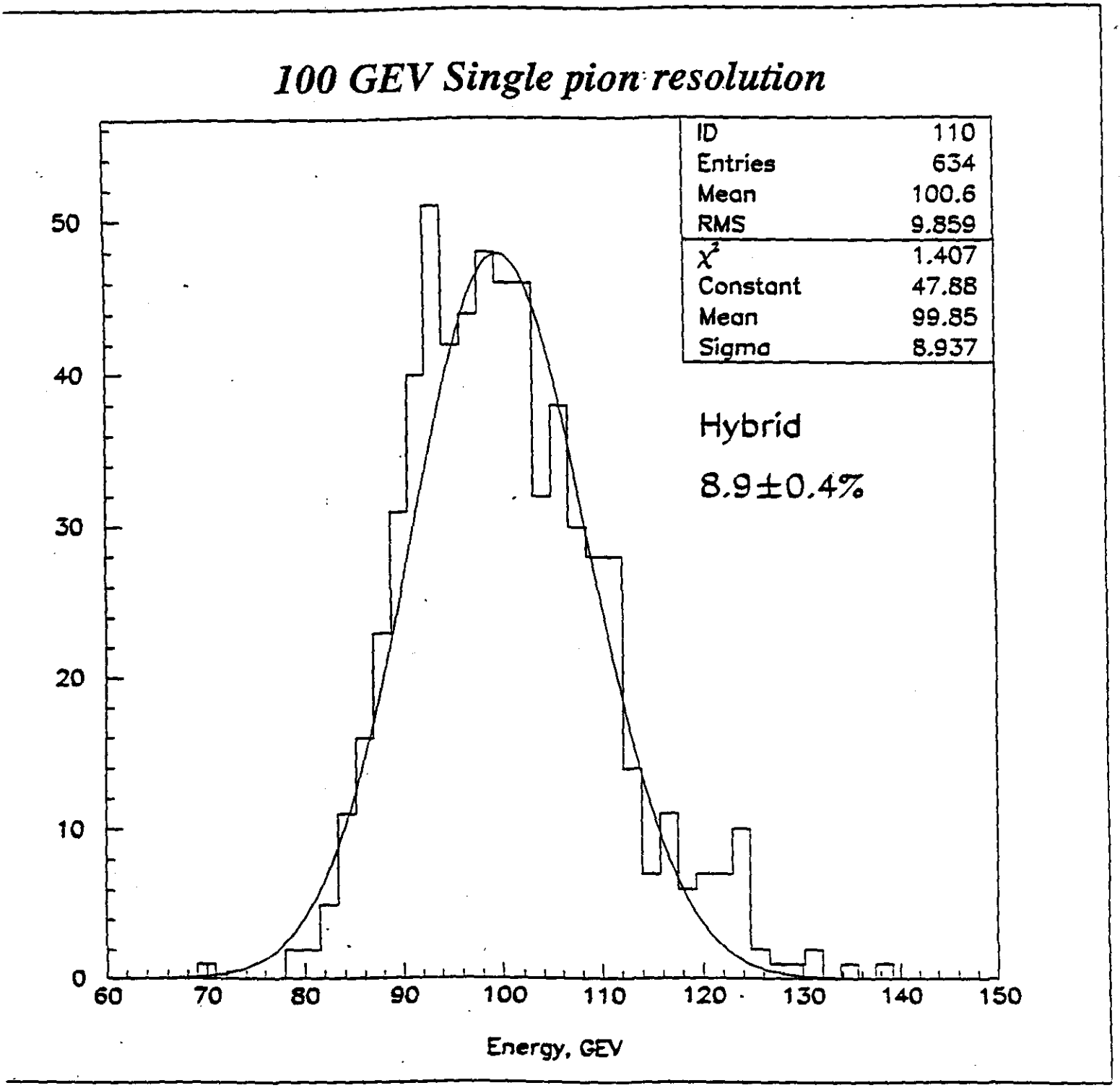
100 GEV Single pion resolution
ID 110
Entries 634
Mean 100.6
RMS 9.859
χ² 1.407
Constant 47.88
Mean 99.85
Sigma 8.937
Hybrid
8.9±0.4%
0
10
20
30
40
50
60
70
80
90
100
110
120
130
140
150
Energy, GEV

Fig 6

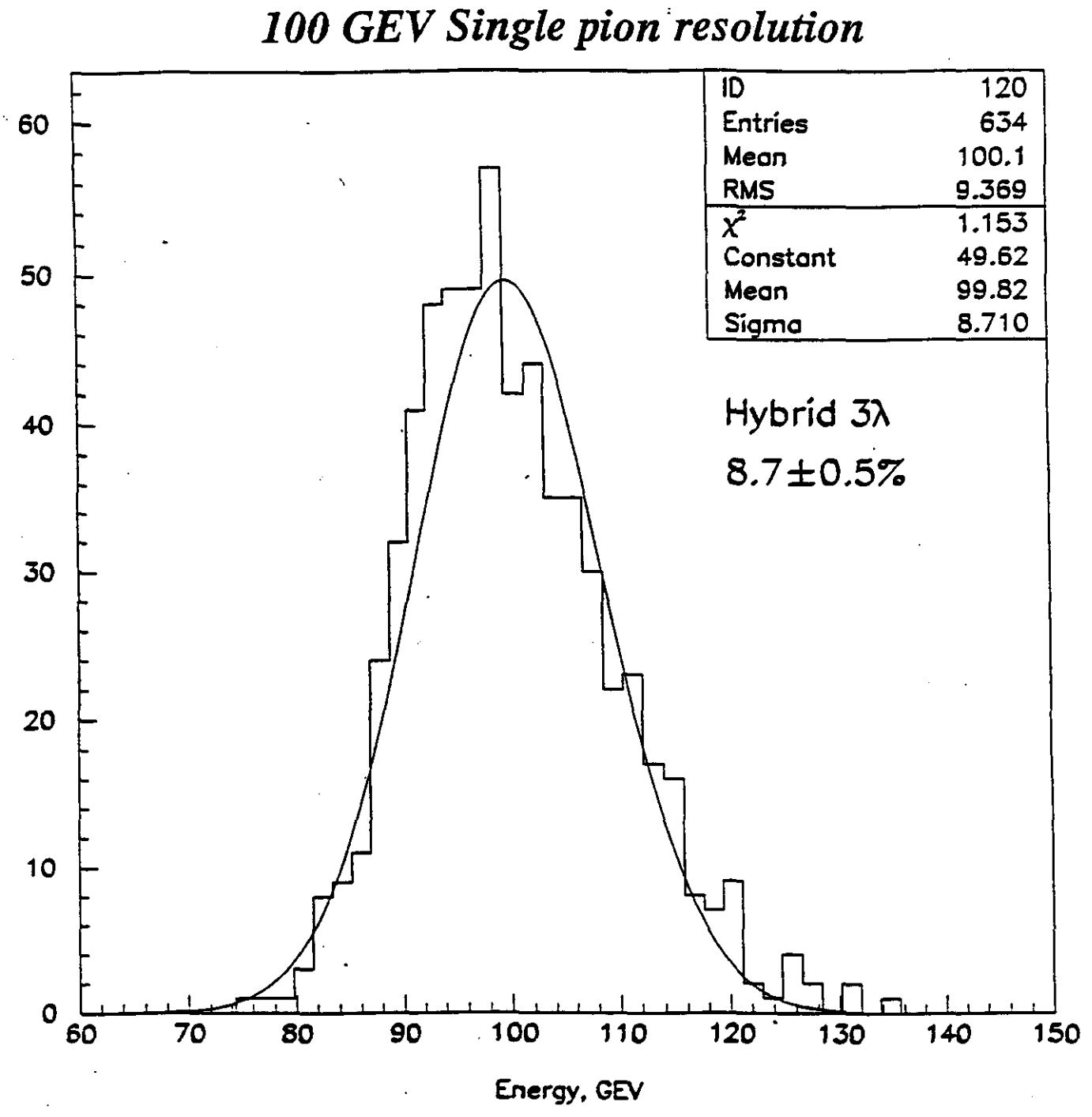
100 GEV Single pion resolution
ID 120
Entries 634
Mean 100.1
RMS 9.369
χ² 1.153
Constant 49.62
Mean 99.82
Sigma 8.710
Hybrid 3λ
8.7±0.5%
0
10
20
30
40
50
60
60
70
80
90
100
110
120
130
140
150
Energy, GEV

Fig 7